INTERFACE

royalsocietypublishing.org/rsif

Research

Cite this article: Park C. 2026 Thermodynamic entropy management in human motor control across circadian and thermal challenges. *J. R. Soc. Interface* **23**: 20251023.
https://doi.org/10.1098/rsif.2025.1023

Received: 5 October 2025
Accepted: 2 April 2026

Subject Category:
Life Sciences–Physics interface

Subject Areas:
systems biology, bioinformatics

Keywords:
thermodynamic entropy, motor variability, circadian rhythm, bimanual coordination, biological adaptation

Author for correspondence:
Chulwook Park
e-mail: pcw8531@snu.ac.kr

Electronic supplementary material is available online at https://doi.org/10.6084/m9.figshare.c.8463251.

THE ROYAL SOCIETY PUBLISHING

Thermodynamic entropy management in human motor control across circadian and thermal challenges

Chulwook Park[1,2,3]

[1]Department of Physical Education, Seoul National University, Seoul, Republic of Korea
[2]Okinawa Institute of Science and Technology (OIST), Okinawa, Japan
[3]International Institute for Applied Systems Analysis (IIASA), Laxenburg, Austria

CP, 0000-0001-8714-5760

The second law of thermodynamics dictates that local decreases in entropy must be offset by increases elsewhere. While this principle is well established in mechanical systems, its role in biological motor control remains underexplored. This study analysed 576 bimanual coordination trials on 16 participants collected across circadian cycles under normal conditions and thermal perturbations to test whether human motor systems strategically regulate functional movement stability. Movement entropy peaked during circadian temperature minima at dawn and declined to its lowest level during temperature maxima in the late afternoon, showing a significant inverse correlation with core body temperature. Thermal perturbations using heat and ice vests amplified these circadian patterns, with cold challenges exerting stronger effects than heat challenges. Despite substantial variations in movement entropy across conditions, task performance in maintaining target phase coordination remained stable. These findings provide preliminary evidence that biological systems can achieve local order through strategic entropy redistribution, increasing movement variability under challenging physiological conditions. The results offer initial empirical support suggesting that human motor control can function as an entropy-management system, revealing how biological systems satisfy thermodynamic laws while preserving functional stability.

1. Introduction

Living organisms perpetually struggle against disorder. Every biological system, from the simplest bacterium to the most complex mammal, must continuously preserve its organized structure against the inexorable drive towards equilibrium dictated by physical laws [1,2]. The fundamental question of how life maintains order in a universe governed by the second law of thermodynamics has captivated scientists since the early twentieth century. Whereas mechanical systems such as air conditioners and heat pumps achieve local order by redistributing entropy according to well-defined engineering principles, biological systems employ more sophisticated strategies that remain only partly understood [3,4].

The second law of thermodynamics imposes fundamental constraints on all energy transformations, whether in engineered systems or biological organisms. In mechanical cycles, formalized by Carnot in 1824 and subsequently adapted for practical applications, heat must be transferred against the natural gradient. The efficiency of such systems, expressed as the coefficient of performance (COP), follows strict thermodynamic limitations:

$$\mathrm{COP} = \frac{Q_c}{W} = \frac{T_c}{T_h - T_c}, \tag{1.1}$$

where Q_c represents the heat removed from the cold reservoir, W is the work input and T_c and T_h are the absolute temperatures of the cold and hot reservoirs, respectively [5]. This process necessarily increases the total entropy, with the work input W driving the heat transfer Q_c from the cold side while rejecting $Q_h = Q_c + W$ from the hot side, ensuring

$$\Delta S = \Delta S_{cold} + \Delta S_{hot} > 0. \tag{1.2}$$

The fundamental thermodynamic principle of entropy exchange can be formalized more generally as

$$\Delta S_{total} = \Delta S_{local} + \Delta S_{environment} \geq 0, \tag{1.3}$$

where any local decrease in entropy ($\Delta S_{local} < 0$) must be compensated by a larger increase in environmental entropy ($\Delta S_{environment} > 0$). Mechanical systems, such as refrigerators and heat pumps, manifest heat generation, friction and energy dissipation throughout the system.

1.1. Biological systems as open thermodynamic entities

The apparent incompatibility between life and thermodynamics remained paradoxical until Ervin Bauer's pioneering work in 1920, when he proposed that 'life is a set of processes that take place in an open nonequilibrium system' [6,7]. This concept was recently re-examined in [8]; it suggests that biological systems necessarily function as open thermodynamic entities to preserve their organized complexity against continuous degradation arising from thermal agitation, which is identified in [9] as the molecular basis for the manifestation of the second law of thermodynamics in living matter.

In the present study, we define the biological system as the motor coordination apparatus (neuromuscular structures controlling bimanual oscillation and their associated neural circuits), which exchanges entropy with the thermal environment comprising the ambient surroundings and (during perturbation conditions) applied thermal vests. Core body temperature (T_{core}) represents the internal thermal state of the system, following the natural circadian rhythm (approximately 36.5–37.1°C across a 24 h cycle).

Living organisms sustain their highly organized states through continuous entropy exchange with their environment, thereby functioning as open thermodynamic systems. Near thermodynamic equilibrium, the entropy production rate can be expressed as

$$\frac{\mathrm{d}S}{\mathrm{d}t} = \sum_i J_i X_i, \tag{1.4}$$

where J_i represents the metabolic flux and X_i represents the conjugate thermodynamic force [10,11]. The minimum entropy production theorem, which states that systems near equilibrium evolve towards states of minimal entropy production, is applicable only under specific conditions such as linear flux–force relationships and standard boundary conditions [3]. The experimental temperature variations (circadian fluctuations of approx. 0.4°C and perturbation-induced changes of approx. 1.2°C) represent a less than 0.5% variation relative to the absolute body temperature (approx. 310 K), which would nominally fall within the near-linear regime. However, biological motor systems typically operate far from equilibrium due to active neural control and metabolic processes, where this theorem does not apply. System behaviour is governed by fundamentally different principles.

For systems which are far from the equilibrium state, Prigogine and co-workers demonstrated that organized 'dissipative structures' can emerge spontaneously through continuous production and export of entropy [12,13]. Such structures maintain their organized structure not by minimizing entropy production, but by efficiently dissipating energy gradients; this principle was later formalized by England [14,15] as 'dissipative adaptation'. The nonlinear-dynamics characteristic of biological coordination reflects this far-from-equilibrium regime. The Haken–Kelso–Bunz (HKB) equation (detailed in §1.3) provides the mathematical formulation

$$\dot{\varphi} = -\partial V(\varphi)/\partial\varphi + \sqrt{\rho}\xi_t, \tag{1.5}$$

where the potential function $V(\varphi) = -a\cos(\varphi) - b\cos(2\varphi)$ generates nonlinear restoring forces creating stable coordination attractors, and the stochastic term $\sqrt{\rho}\xi_t$ represents thermal fluctuations driving the system away from these attractors. Critically, this formulation connects to far-from-equilibrium thermodynamics through the fluctuation–dissipation relationship: the noise amplitude ρ is not merely a random perturbation but reflects the system's coupling to the thermal degrees of freedom [16,17]. The entropy production rate in such driven systems scales with the dissipation required to maintain coordination against fluctuations:

$$\dot{S} \propto \rho \cdot |\partial V/\partial\varphi|^2. \tag{1.6}$$

Thus, regions of the coordination landscape requiring stronger restoring forces (steeper potential gradients) necessarily involve greater entropy production. This nonlinear coupling between potential landscape and dissipation, which is absent in linear near-equilibrium theory, enables the emergence of stable coordination patterns as dissipative structures. The temperature-dependent modulation of $\rho(T)$ proposed in §1.4 provides the mechanism by which circadian and thermal challenges influence entropy management through this dissipative process.

Building on these thermodynamic foundations, we propose that biological motor systems follow an analogous principle of entropy management, which is the process by which motor systems redistribute variability across different degrees of freedom to maintain functional stability under physiological challenges. This relationship can be expressed as

$$\Delta S_{biological} = \Delta S_{task} + \Delta S_{movement} \geq 0, \tag{1.7}$$

where ΔS_{task} represents the entropy associated with maintaining the target coordination pattern (low values indicating stable, consistent performance with minimal deviation from the intended phase relationship) and $\Delta S_{movement}$ represents the distributional variability of movement patterns quantified through phase distribution uncertainty. According to this model, maintaining low task entropy under challenging conditions requires compensatory increases in movement entropy. We emphasize that this approach employs thermodynamic concepts as a guiding analogy: Shannon entropy of phase distributions $H(\varphi)$, which is used as the empirical measure, quantifies informational uncertainty in movement patterns. This serves as a functional proxy paralleling thermodynamic entropy, conceptually [18]. The value of this analogy lies in reframing motor variability not as noise or degradation, but as a potentially adaptive mechanism for maintaining functional stability under physiological challenges in a manner which is analogous to how refrigerators achieve local cooling through global heat dissipation. This principle is tested empirically through the experiments described herein.

1.2. Homeostasis as cybernetic management of thermodynamic constraints

As emphasized in [8], the compatibility of living organisms with thermodynamic constraints is possible because life is subject to cybernetic requirements arising from evolution. Building on Claude Bernard's concept of *le milieu intérieur* and Walter Cannon's formalization of homeostasis [19], Ross Ashby developed a mathematical formulation demonstrating that biological systems maintain 'essential variables' within narrow ranges through adaptive control mechanisms [20]. Ashby's suggestion, which was later synthesized in dynamics [21], establishes that survival requires mapping:

$$\Gamma: P^{*}S \rightarrow S, \tag{1.8}$$

where S represents all the system states and P represents the contextual parameters. This cybernetic control operates through the term 'information catalysts' ($iCat$)

$$iCat = \left[I_{input}{}^{*}I_{output}\right], \tag{1.9}$$

where I_{input} filters relevant patterns from environmental and proprioceptive signals and I_{output} channels the responses towards goal-directed actions [8]. These information catalysts represent biological implementations of 'Maxwell's demons', which are entities that use information to create local order. This was first proposed for biological systems [22] and later developed in hierarchical organization [23].

1.3. Circadian rhythms and elementary (motor) coordination dynamics

The circadian rhythm exemplifies thermodynamic principles at the organism level. Core body temperature (T_{core}), which is the internal thermal state of an organism measured via infrared tympanic thermometry, oscillates predictably between approximately 36.6°C at 05.00 (the circadian minimum) and 37.0°C at 17.00 (the circadian maximum). This oscillation is driven by suprachiasmatic nuclei regulation of metabolic rate and thermoregulatory set points [24,25] and constitutes a natural perturbation that challenges motor control systems, creating conditions analogous to those of a heat pump operating under varying temperature differentials during the day. This regulation is evolutionarily conserved across kingdoms; plants such as *Arabidopsis thaliana* exhibit temperature compensation mechanisms that maintain constant circadian periodicity despite changes in the environmental temperature [26], suggesting that these principles may reflect fundamental thermodynamic constraints on biological timing systems.

Circadian temperature variation reflects the organism's management of what were identified in [8] as three key constraints that living beings must satisfy to cope with thermodynamic demands: homeostasis, teleonomy (a purpose-oriented structure without a designer as distinguished from teleology) and goal-directed information processing. The mathematical basis for understanding biological motor control in this thermodynamic context is derived from the HKB model of coordination dynamics. The original HKB equation describes the evolution of the relative phase ϕ between coupled oscillators as

$$\dot{\phi} = \Delta\omega - \alpha\sin(\phi) - 2b\sin(2\phi) + \sqrt{\varrho}\xi_t, \tag{1.10}$$

where $\Delta\omega$ represents frequency difference, α and b are coupling parameters determining the stability of in-phase ($\phi = 0$) and anti-phase ($\phi = \pi$) coordination modes and $\sqrt{\varrho}\xi_t$ represents Gaussian white noise [27,28]. The potential function defining the attractor landscape is

$$V(\phi) = -\alpha\cos(\phi) - b\cos(2\phi), \tag{1.11}$$

with local minima at stable coordination patterns.

1.4. Thermodynamic extension: symmetry breaking through temperature coupling

To incorporate thermodynamic influences, the model was extended by introducing thermal coupling terms that represent the symmetry-breaking effects of circadian temperature variations [29]. Following the experimental design, the modified dynamics are expressed as

$$\dot{\phi} = \Delta\omega - [\alpha\sin(\phi) + 2b\sin(2\phi)] - \left[c\sin\left(\phi^T\right) + 2d\sin\left(2\phi^T\right)\right] + \sqrt{\varrho}\xi_t\,. \tag{1.12}$$

Here, the thermal coupling terms $[c\sin(\phi^T) + 2d\sin(2\phi^T)]$ represent the system's entropy-management response to circadian temperature (ϕ^T = temperature-modulated phase, not phase to the power of T) variations, whereas the noise term $\sqrt{\varrho}\xi_t$ captures the increase in adaptive variability necessary to maintain the entropy balance $\Delta S_{biological} \geq 0$. These terms mathematically implement the biological entropy-management model; c quantifies coupling to the circadian temperature cycle, d represents coupling to core body temperature dynamics and ϱ denotes the temperature-dependent noise amplitude reflecting the system's adaptive entropy redistribution. This symmetry-breaking mechanism emerges when the coupling conditions satisfy

$$|c| > 0 \quad \text{and} \quad |d| > 0 \tag{1.13}$$

rather than the symmetric case where $|c| \approx 0$ and $|d| \approx 0$, which would preserve perfect environmental synchronization [30].

To clarify the theoretical architecture of this study, we integrate three complementary approaches that serve distinct roles: (i) non-equilibrium thermodynamics provides the conceptual motivation: biological systems must manage entropy exchange with their environment to maintain organized function; (ii) the nonlinear HKB model provides the dynamic basis, capturing the attractor dynamics of coordination and generating the stable patterns observed through dissipative structures; and (iii) Shannon information entropy provides the measurement approach that quantifies distributional uncertainty in phase patterns as an empirically accessible variable. We do not claim that these constitute a unified thermodynamic theory of motor control; such unification remains an important challenge for future theoretical work. Rather, we propose that the principle of entropy management, where local order is achieved through distributed variability, operates in biological coordination, with Shannon entropy serving as a tractable empirical proxy for this organizational principle. The experiments that follow test whether the behaviour of this proxy measure is consistent with thermodynamic predictions.

1.5. Information-theoretic quantification of movement entropy

From information theory, we quantify movement entropy $H(\phi)$—the Shannon information entropy of the relative phase distribution between oscillating limbs—using the standard formulation:

$$H(\phi) = -\sum_i p_i \log p_i, \tag{1.14}$$

where p_i represents the probability of observing phase states within discretized bins sampled over time windows [31]. This measure, expressed in bits, quantifies the distributional uncertainty of coordination patterns: higher values indicate greater movement variability (more uniformly distributed phases), while lower values indicate more concentrated, predictable phase relationships clustered near the target coordination state. The entropy $H(\phi)$, then, corresponds to the $\Delta S_{movement}$ term in the biological entropy-management model, quantifying the variability component that compensates for reduced task entropy ΔS_{task}, connecting to the Woodward–Kharkevich information value, which is emphasized as crucial for biological systems:

$$J(d, T) = \log[P(d, T)/P(\theta, T)], \tag{1.15}$$

where positive J indicates information that brings the system closer to the target T, whereas negative values represent 'disinformation' that increases entropy without improving task performance [32,33].

At circadian temperature minima (05.00), the thermoregulatory system operates under conditions of reduced metabolic heat production and diminished neural efficiency associated with the circadian trough [24]. The biological challenge at this time arises from reduced physiological capacity rather than thermal gradients *per se*; the system operates closer to its lower regulatory boundary with diminished homeostatic reserve. This is reflected in increased movement entropy, representing an adaptive response to maintain essential motor variables within viable ranges despite compromised operating conditions.

1.6. Research gap: entropy management in motor control

Although extensive research has examined the effects of circadian rhythms on motor performance [34–36] and coordination dynamics under various conditions [27,28,37], previous studies have not explicitly linked these phenomena to thermodynamic entropy-management principles. Three critical gaps remain in the literature.

First, although circadian effects on reaction time, strength and coordination accuracy are well documented [38–40], these studies treat performance variations as simple degradation rather than potential adaptive strategies. No study has examined whether increased movement variability at circadian temperature minima represents strategic entropy redistribution rather than a mere decline in performance. Second, although the HKB model and its extensions have successfully described coordination dynamics under various perturbations [41–43], these models do not incorporate thermodynamic constraints or entropy management as organizing principles. The potential role of temperature-dependent coupling in coordination stability remains unexplored. Third, despite growing interest in variability as a functional aspect of motor control [44–46], no studies have quantified movement variability as entropy in an information-theoretic sense or linked it to the thermodynamic requirements of homeostasis. The relationship between the Shannon entropy of movement patterns and biological entropy management has not been empirically established.

1.7. Empirical predictions: entropy management through variability

The proposed thermodynamic model generates three testable predictions addressing the following gaps. (i) Movement entropy $H(\phi)$ should be highest under the most challenging physiological conditions, specifically at circadian temperature minima (05.00). This prediction derives from established findings that motor performance parameters vary systematically with circadian phase [34,39] and directly tests whether biological systems increase movement variability as a compensatory mechanism when physiological efficiency is lowest [24]. (ii) External thermal perturbations (heat or ice vests) amplify entropy-management strategies, producing significant interaction between circadian phase and thermal manipulation. This prediction extends previous work demonstrating that coordination dynamics are sensitive to physiological perturbations [41,43] and tests whether the motor system actively adjusts its entropy distribution in response to thermodynamic challenges. (iii) Despite increased movement entropy at temperature extremes, task-level performance (maintaining target phase relationships) should remain stable through strategic variability distribution. This prediction aligns with the uncontrolled manifold hypothesis [47] and optimal variability frameworks [44], distinguishing adaptive entropy management from simple performance degradation.

Our hypothesis is that biological motor systems achieve stable task performance through strategic entropy redistribution, following the principle

$$H(\phi) \propto 1/T_{core}\,. \tag{1.16}$$

This inverse relationship between movement entropy and core temperature arises from the thermodynamic requirement that entropy production must increase when the system operates outside its optimal temperature range. This relationship follows directly from our entropy-management model, $\Delta S_{biological} = \Delta S_{task} + \Delta S_{movement} \geq 0$, in which decreased physiological efficiency at temperature extremes necessitates increased movement entropy to maintain the inequality while preserving task stability. The motor system functions as a catalyst for biological information, processing sensory input to guide thermodynamically favourable coordination while managing entropy distribution to sustain functional stability [48].

The experimental paradigm of bimanual coordination provides an ideal testbed for the theoretical predictions. At core body temperature minima (05.00), the system experiences maximal thermodynamic stress, requiring what Ashby [49] termed 'ultrastability', the capacity to maintain essential variables despite perturbations. By applying thermal challenges via heat and ice vests, it is possible to determine whether increased movement variability functions as a compensatory mechanism, implementing the cybernetic control necessary for homeostasis under thermodynamic constraints. This study provides the first empirical observation of thermodynamic entropy management in human motor control. The findings have implications beyond motor neuroscience, potentially enhancing our understanding of biological adaptation [50], movement disorders [51,52] and the fundamental principles underlying resistance of human life to thermodynamic decay. If biological systems are able to manage entropy, as our model suggests, it would constitute a unifying principle linking physics, cybernetics and biology, revealing how the same thermodynamic laws that govern heat engines also shape the elegant variability of human movement [53,54].

2. Methods

2.1. Participants and ethical considerations

The dataset comprised 576 observations from 6 bimanual coordination trials each on 16 healthy adults who participated in this study, which investigated the thermodynamic principles of biological motor control. Participants were divided into two groups of eight. The first group (six males, two females; mean age 25 ± 3 years) completed all the experiments under normal temperature conditions (Experiment I). The second group (six males, two females; mean age 25 ± 3 years) underwent thermal perturbation protocols, experiencing both heat and cold vest conditions in Experiments II and III, respectively. This design allowed between-group comparisons of thermal effects while maintaining within-subject comparisons for circadian variations and for different thermal challenges in the perturbation group. All participants were right-handed, had normal or corrected-to-normal vision and reported no history of neurological or musculoskeletal disorders affecting bimanual coordination. Written informed consent was obtained from all the participants in accordance with protocols approved by the Seoul National University Institutional Review Board (SNUIRB no. 1509/002-002), conforming to the ethical standards of the 1964 Declaration of Helsinki (Report ID: 20481572).

The within-subject repeated-measures design substantially reduces between-subject variability, with the total dataset comprising 576 observations (16 participants × 6 trials × 4 conditions). This sample size aligns with that of other coordination dynamics studies employing similar paradigms [28,55]. *Post hoc* power analysis (*G*Power* 3.1) [56] confirmed statistical adequacy: the achieved power ranged from 0.82 to 0.89 across experiments, with all effect sizes exceeding the threshold for large effects ($\eta^2 p = 0.32 - 0.38$) [57]. Complete power analysis details, bootstrap confidence intervals (CIs) and sensitivity analyses are provided in the electronic supplementary material, S8. Core body temperature was measured at each experimental time point rather than relying on assumed circadian peaks, allowing verification of circadian phase alignment (see §3.1).

2.2. Experimental design and theoretical rationale

The experimental design was developed to test the biological entropy-management model proposed in our theoretical rationale, specifically assessing whether the relationship $\Delta S_{biological} = \Delta S_{task} + \Delta S_{movement} \geq 0$ is maintained across varying thermodynamic

challenges. In the three experiments, the circadian phase and thermal conditions were systematically manipulated to investigate the motor system's strategies for entropy redistribution.

Experiment I established baseline circadian effects on movement entropy by sampling coordination dynamics across the full circadian cycle in all eight participants of Group 1 (see table 1). This experiment examined whether ecological temperature cycles influence biological motor systems, testing the hypothesis that movement entropy inversely correlates with core body temperature and follows the $H(\phi) \propto 1/T_{core}$ law.

Experiments II and III employed a mixed design combining between-group comparisons (normal versus perturbation groups) with within-subject comparisons across circadian times (05.00 versus 17.00). Thermal perturbations were applied at circadian extremes [58], testing whether external thermal challenges amplify entropy-management strategies. Using the same perturbation group for both heat and cold conditions allowed direct within-subject comparisons of bidirectional thermal effects.

2.3. Apparatus and instrumentation

The experimental apparatus comprised two identical pendulum systems designed to probe coordination dynamics (table 2). The configuration yielded a natural oscillation period of approximately 1.21 s, chosen to facilitate resonant oscillations when coupled with metronome pacing [55]. Temperature measurements were recorded continuously throughout the experimental sessions to verify perturbation effectiveness and monitor recovery dynamics. All the experiments were conducted under standard laboratory conditions in a university department building within a fixed experimental period during late spring to ensure consistent environmental circadian conditions across all participants. This seasonal constraint maintained reliable photoperiod and ambient thermal patterns while preserving the natural diurnal variation essential to the research question. Complete experimental datasets, including all individual participant entropy values and core body temperature measurements reported in the electronic supplementary material, tables S1–S3, are publicly available in the GitHub online repository (https://github.com/pcw8531/thermodynamic-motor-control) to facilitate independent verification and replication efforts.

2.4. Experimental procedures

The participants were seated comfortably, with their forearms voluntarily stabilized to constrain pendulum motion to the sagittal plane, ensuring oscillations occurred at the single joints, whereas the other joints remained immobile. Vision was not occluded to maintain ecological validity and natural coordination. Before data collection, the participants received standardized instructions: swing both pendulums together in synchrony at a pace indicated by the metronome. Maintain smooth, continuous oscillations without letting the pendulums slip and without rotating the wrists. Participants were naive to the specific study hypotheses throughout the data collection process. The informed consent and verbal instructions described the study as an investigation of 'bimanual coordination under different time-of-day and temperature conditions' without reference to entropy, thermodynamics or predicted directional effects. This blinding procedure minimized potential demand characteristics. Importantly, the primary dependent measure, namely Shannon entropy of relative phase distributions, is computed from objective kinematic recordings of the angular displacement of the pendulum. These distributional properties emerge from biomechanical constraints and coordination dynamics rather than volitional control; participants could not consciously manipulate phase distribution entropy even if motivated to do so. Upon completion of all the experimental sessions, the participants were debriefed regarding the study objectives in accordance with ethical guidelines.

Each experimental session began with a baseline core temperature recording, followed by three practice trials to ensure task comprehension. During data collection, an auditory metronome provided pacing at 1.21 s intervals to establish in-phase ($\phi = 0^{\circ}$) coordination with 1 : 1 frequency locking. Each trial lasted 60 s, generating approximately 50 oscillation cycles, with 5 min rest intervals between trials. This work–rest ratio was selected based on previous research demonstrating the maintenance of the thermal state under these conditions [59]. For the thermal perturbation experiments (II and III), the perturbation group underwent a 30 min application of heat (Experiment II) or ice (Experiment III) vests, whereas the normal group remained in ambient temperature conditions. The core body temperature was measured at three time points: (i) baseline, before vest application; (ii) immediately after the 30 min vest application period, to verify target perturbation magnitudes; and (iii) following data collection, to assess temperature maintenance. Temperature verification after vest application confirmed that the target perturbations were achieved: heat condition +1.3 ± 0.1°C above baseline (range: +1.2 to +1.5°C across participants), cold condition −1.2 ± 0.1°C below baseline (range: −1.0 to −1.4°C across participants). Data collection commenced within 5 min of temperature verification to capture maximum perturbation effects, and all the trials were completed within 30 min of vest removal to prevent temperature normalization towards the baseline [60]. Temperature monitoring continued throughout the rest periods to track the recovery dynamics and to ensure participant safety. The complete temperature time courses, including adaptation curves during vest application and recovery profiles after removal, are documented in figure 1 and electronic supplementary material, S3.

2.5. Data processing and phase dynamics quantification

Angular displacement data from the direct current (DC) angular position sensor potentiometers were sampled at 100 Hz and processed using a fourth-order Butterworth low-pass filter with a 10 Hz cut-off frequency to remove high-frequency noise while preserving movement dynamics. The continuous relative phase between the left and right pendulums was computed using an established coordination dynamics methodology [61]:

Table 1. Experimental design summary.

experiment	condition	participants (*N*)	circadian points	trials per point	independent variables	dependent variables
I	normal	group 1 (8)	05.00, 12.00, 17.00, 00.00	6	circadian time (4 levels)	$H(\phi)$, SD_ϕ, $\phi_{ave} - \phi_0$
II	normal	group 2 (8)	05.00, 17.00	6	circadian time (2 levels) × temperature (normal versus heat)	$H(\phi)$, SD_ϕ, $\phi_{ave} - \phi_0$
	heat-perturbed		05.00, 17.00	6		
III	normal		05.00, 17.00	6	circadian time (2 levels) × temperature (normal versus cold)	$H(\phi)$, SD_ϕ, $\phi_{ave} - \phi_0$
	cold-perturbed		05.00, 17.00	6		

Note: $H(\phi)$ = movement entropy; SD_ϕ = phase variability; $\phi_{ave} - \phi_0$ = fixed-point shift from intended coordination pattern. The perturbation group participated in both hot and cold conditions, allowing within-subject comparisons of different thermal challenges.

Table 2. Specifications of experimental apparatus.

equipment	specification	purpose
pendulum rods	wooden, 100 cm length, 1.2 cm diameter, 85 g mass	oscillation apparatus
pendulum weights	200 g, positioned 30 cm from base	eigenfrequency calibration ($T = 1.21$ s)
grip position	standardized at 60 cm from base	consistent mechanical properties
DC potentiometers	resolution 0.25°, sampling rate 100 Hz	continuous angular displacement measurement
digital metronome	1.21 s period (0.83 Hz)	auditory pacing signal
infrared thermometer	HuBDIC HFS-100, non-contact, medical-grade	core body temperature measurement
heat vest	ThermaCare, 42–45°C surface temperature, 30 min application	heat perturbation protocol
cold vest	CoolVest with gel packs, 5–10°C surface temperature, 30 min application	cold perturbation protocol

$$\phi = \theta_L - \theta_R, \tag{2.1}$$

where θ_L and θ_R represent the instantaneous angular positions of the left and right pendulums, respectively. The degree of the relative phases (0°–180°) depends on the difference between the two oscillators. If each θ was defined as a sine function, as follows:

$$\theta_1 = \omega_1 - \frac{\alpha}{2}\sin(\theta_1 - \theta_2), \tag{2.2}$$

$$\theta_2 = \omega_2 - \frac{\alpha}{2}\sin(\theta_2 - \theta_1), \tag{2.3}$$

the logic can simply be rewritten to ϕ as the same dynamic function:

$$\theta_1 - \theta_2 = \phi\,. \tag{2.4}$$

Then, each θ can be specified using the following equations:

$$\left.\begin{aligned}\dot{r} &= 0\\ \dot{\theta} &= \omega\end{aligned}\right\} \Rightarrow\ \theta(t) = \omega t + \theta(0), \quad \begin{aligned}\theta_1 &= \omega_1 = \theta_1(t) = \omega_1(t) + \theta_1(0)\\ \theta_2 &= \omega_2 = \theta_2(t) = \omega_2()t) + \theta_2(0)\end{aligned} \tag{2.5}$$

$$\phi = \theta_2 - \theta_1 = \omega_2 - \omega_1 = \Delta\omega(t) + \phi(0) = \phi(t)\,. \tag{2.6}$$

To derive the relative phase time series of both hands, it was necessary to identify the maximum extensions from the three-dimensional data collected via the DC potentiometers. Although the data were relatively regular, as participants were instructed to maintain in-phase 1 : 1 frequency locking at the 1.21 s metronome beat, principal component analysis was applied to reduce the three-dimensional data to a one-dimensional representation.

First, the data from both hands were separated into left and right components. Each set was then reduced to its peak points (left_peaks and right_peaks) to form a one-dimensional dataset, with each peak associated with its corresponding time vector. These peak sets were subsequently analysed using a discrete relative phase formula as follows:

$$\phi_i = 2\pi\frac{t_{max}L_i - t_{max}R_i}{t_{max}L_{i+1} - t_{max}L_i}, \tag{2.7}$$

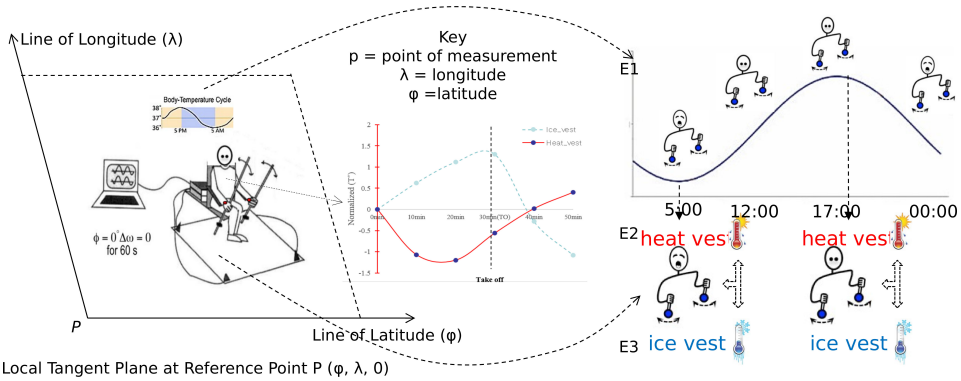

Figure 1. Schematic drawing of the experimental setting and conditions. Left: general experimental setting. Upper right: experimental design 1. Bottom right: experimental design 2 (normal versus abnormal conditions). For each experiment (E1, E2 and E3), every participant was required to be present four times with six trials each time (one participant, 1 min, 24 trials = 6 [trials] × 4 [different time points = T1–T4]). Middle plots show an illustration of the temperature according to the experimental design. The horizontal axis denotes the temperature check time (T0 = take off the ice/heat vest under the perturbation condition). The vertical axis is the level of the temperature change as calculated in Fahrenheit (°F) and Celsius (°C). Note that in the abnormal session, the data were collected after 30 min (from 30 to 60 min) of taking the heat = E2 (or ice = E3) vest off, whereas in the normal session, the data were collected after 30 min without taking the ice (or heat) vest off to ensure that the conditions were identical.

where $t_{max}L_i$ is the time of the i maximum extension of the left pendulum. This discrete formulation captures the cycle-by-cycle variations in coordination, which are essential for entropy quantification (see electronic supplementary material, S1, for detailed calculation procedures and exclusion criteria, with computational implementations and sample raw data available in our open repository: https://github.com/pcw8531/thermodynamic-motor-control, files: phase_analysis.py, cwa17w1.txt).

2.6. Entropy quantification and thermodynamic modelling

Movement entropy was quantified using Shannon's information entropy applied to the probability distribution of the observed phase states:

$$H(\phi) = -\sum_i p_i \log p_i, \tag{2.8}$$

where p_i represents the probability of observing the phase states within discretized bins of width $\pi/20$ rad. This measure quantifies the distributional complexity of coordination patterns, with higher values indicating greater movement variability corresponding to increased $\Delta S_{movement}$ in the theoretical model. The entropy calculation directly operationalizes the biological entropy-management principle, enabling empirical testing of whether increased movement entropy compensates for thermal challenges to maintain task stability (see electronic supplementary material, S1.2, for complete entropy quantification methodology, with full computational implementation available in our open repository: https://github.com/pcw8531/thermodynamic-motor-control, file:Analysis.py).

Shannon entropy was selected as the primary variability measure for four reasons: (i) it captures the full distributional complexity of phase patterns (quantifying how uniformly or narrowly distributed the phases are across the coordination space) rather than merely measuring dispersion around a central tendency as standard deviation does; (ii) it is scale-independent and directly comparable across experimental conditions without requiring normalization; (iii) it has established precedent in coordination dynamics and motor control research [46,55,62]; and (iv) it provides conceptual linkage to thermodynamic entropy through information theory, enabling the theoretical linkage connecting motor variability to physical principles [18,31]. Alternative nonlinear measures, such as sample entropy and multiscale entropy, could provide complementary insights regarding the temporal structure and are identified as directions for future investigation.

A modified HKB equation incorporating thermal coupling was then implemented to model the observed dynamics, as follows:

$$\dot{\phi} = \Delta\omega - [\alpha\sin(\phi) + 2b\sin(2\phi)] - \left[c\sin\left(\phi^T\right) + 2d\sin\left(2\phi^T\right)\right] + \sqrt{\varrho}\xi_t\,. \tag{2.9}$$

The terms $[c\sin(\phi^T) + 2d\sin(2\phi^T)]$, here, denote the system's entropy-management response to circadian temperature variations, where c quantifies coupling strength to the environmental circadian cycle and d represents coupling to core body temperature dynamics. The temperature-dependent noise amplitude ϱ captures adaptive variability increases necessary to maintain the thermodynamic inequality $\Delta S_{biological} > 0$. This formulation extends the standard HKB model by incorporating temperature as a symmetry-breaking parameter (see electronic supplementary material, S1.3), with $|c| > 0$ and $|d| > 0$ indicating a deviation from perfect environmental synchronization (model validation and parameter fitting are detailed in electronic supplementary material, S7).

2.7. Normal and abnormal day–night circadian temperature perturbations

There is a state of unit x at time t denoted by $x(t)$, which represents the ensemble average of the system. Collective behaviour emerges from a homogeneous state when a parameter undergoes transition from $x = 0$ to $x \neq 0$. To reflect this transition in terms of an external parameter, the temperature perturbation is formalized as

$$\varepsilon(\chi, t) = T(\chi, t) - T_0(t), \tag{2.10}$$

where ε represents the control parameter quantifying the deviation from baseline conditions, $T_0(t)$ is the baseline core body temperature at time t and $T(\chi, t)$ is the perturbed temperature state. The effective control parameter T_0 serves as a reference to measure the distance of ε with respect to the unperturbed thermal state. This formulation distinguishes between baseline and perturbed thermal states: when $|\varepsilon| \approx 0$, the system operates under normal circadian conditions; when $\varepsilon > 0$ (core temperature elevated above baseline), the system experiences heat perturbation; when $\varepsilon < 0$ (core temperature depressed below baseline), the system experiences cold perturbation. The term 'unstable' here refers to the deviation from the expected circadian thermal trajectory rather than dynamical instability in the mathematical sense. This temperature-perturbation formulation operationalizes the thermodynamic variable beyond conventional measures such as mean internal energy and entropy, enabling quantification of how biological systems redistribute entropy in response to thermal challenges. The distance $|T(\chi, t) - T_0(t)|$ directly relates to the magnitude of entropy reorganization required to maintain task stability, as predicted by the biological entropy-management model ($\Delta S_{task} + \Delta S_{movement} \geq 0$).

This temperature perturbation is interpreted as a thermodynamic variable; it is not limited to conventional thermodynamic measures such as mean internal energy or entropy. As shown in figure 1, the emergence of collective behaviour, reflected by the increasing distance between $T(\chi, t) - T_0(t)$ under perturbation, corresponds to an increase (or decrease) in entropy. Comparing states with $T_0 < \epsilon$ and $T_0 > \epsilon$ (see electronic supplementary material, S3, figures S2.1 and 2.2), as the distance to the ordered state decreases, the peak in entropy production rate increases. It is important to note that the biological non-equilibrium bias towards a particular temperature component suggests a potential link between physical stability and entropy production. Considering the entropy production embedded within the order–disorder biophysical dynamics, differences between the two circadian rhythm points (AM and PM, representing a nearly 24 h oscillatory variation) and the two temperature conditions were compared against psychomotor vigilance (i.e. $\dot{\phi}$ biological motor stability) to determine whether variations in biological disorder correspond to differences in environmental perturbations.

2.8. Statistical analysis

Statistical analyses were conducted to determine whether movement entropy patterns supported the predictions of the thermodynamic basis. In Experiment I, eight participants (Group 1) were assessed using a one-way repeated-measures analysis of variance (ANOVA) to test circadian effects (four levels: 05.00, 12.00, 17.00 and 00.00) on entropy production, phase variability and fixed-point shift. *Post hoc* comparisons were performed using paired t-tests with Bonferroni correction (adjusted $\alpha = 0.0125$) to control the family-wise error rate.

Experiments II and III employed two-way repeated-measures ANOVAs with eight participants (Group 2) completing both normal baseline and thermal perturbation conditions. In Experiment II, the within-subject factors were temperature condition (normal versus heat-perturbed) and circadian time (05.00 versus 17.00). Similarly, Experiment III examined temperature condition (normal versus cold-perturbed) and circadian time as within-subject factors. This design allowed each participant to serve as their own control, thereby eliminating between-subject variability in assessing thermal responses. F-statistics were computed as the ratio of mean squares:

$$F_{temperature} = \frac{MS_{temperature}}{MS_{error}}, \quad F_{circadian} = \frac{MS_{circadian}}{MS_{error}}, \quad F_{interaction} = \frac{MS_{temperature * circadian}}{MS_{error}}. \tag{2.11}$$

These analyses directly tested whether thermal perturbations amplified circadian entropy-management strategies, as predicted by the symmetry-breaking mechanism in the modified coordination dynamics. Statistical significance was set at $\alpha = 0.05$, with partial η^2 reported as the effect size. Normality assumptions were verified using Shapiro–Wilk tests, and sphericity was assessed with Mauchly's test, applying Greenhouse–Geisser corrections when violations occurred. All statistical analyses were conducted using SPSS (IBM Corp., Armonk, NY, USA; see electronic supplementary material, S6, for complete outputs and *post hoc* comparisons). All raw data underlying the statistical analyses are provided in the online repository to ensure full transparency and reproducibility of the reported findings.

2.9. Data quality and availability

Rigorous exclusion criteria ensured data quality. Trials exhibiting phase wandering exceeding 2π radians, amplitude asymmetry greater than 30% between limbs and frequency deviations exceeding 15% from metronome pace were excluded. These criteria (illustrated in electronic supplementary material, S2, figure S1) led to the exclusion of five participants during pilot testing, resulting in a final sample of 16 participants with complete datasets.

To ensure full reproducibility, all experimental data and analysis code are openly available at https://github.com/pcw8531/thermodynamic-motor-control under MIT licence (https://doi.org/10.5281/zenodo.19201270). The repository contains self-contained Jupyter notebooks with embedded data enabling complete reproduction of all analyses and figures, along with raw

time-series data and Python package requirements. Statistical analyses were conducted using SPSS v. 27 with verification performed using Python. Repository structure and variable descriptions are detailed in electronic supplementary material, S9.

3. Results

3.1. Circadian entropy exchange in normal conditions

Analysis of movement entropy across the circadian cycle revealed significant temporal variations in bimanual coordination tasks. Individual entropy patterns showed substantial circadian modulation (see electronic supplementary material, S4.1, table S1, for complete raw data), with distinct profiles across participants (see electronic supplementary material, S2, for further details). Movement entropy varied markedly during the 24 h cycle, ranging from 2.882 (P1 at 12.00) to 5.888 (P4 at 12.00). Importantly, verification of individual temperature patterns confirmed consistent circadian phase alignment across all the participants. Participants (8/8, 100%) exhibited their temperature maximum at 17.00 and minimum at 05.00, with no individual showing reversed or phase-shifted patterns. The mean circadian amplitude was 0.45 ± 0.09°C (range: 0.4–0.6°C), consistent with established norms for healthy adults [24]. A paired t-test comparing temperatures at circadian extremes confirmed that this pattern was highly significant ($t(7) = 13.75$, $p < 0.001$, Cohen's $d = 4.35$). This uniformity in circadian phase, despite the absence of chronotype screening, strengthens confidence that the observed entropy–temperature relationships reflect genuine thermodynamic coupling rather than artefacts of individual circadian variation.

At the group level, movement entropy exhibited clear circadian modulation, peaking at 05.00 (mean $H(\phi) = 5.246$) when core body temperature was lowest (36.575°C), and decreasing at 17.00 (mean $H(\phi) = 4.544$) when the temperature reached its maximum (37.023°C; figure 2, left). This inverse relationship was consistent across multiple analytical approaches. The distribution of entropy values showed greater variability during low-temperature periods (figure 2, middle), with the 05.00 time point displaying both the highest median entropy and the widest interquartile range. Conversely, the 17.00 time point exhibited the most constrained entropy distribution, indicating tighter motor control under optimal physiological conditions. Correlation analysis between core temperature and movement entropy across all measurements confirmed a negative relationship (figure 2, right), supporting the theoretical prediction . This thermodynamic coupling was evident despite individual differences in absolute entropy values. The observed patterns support the proposed biological entropy-management model (complete ANOVA tables in electronic supplementary material, S6.1) where $\Delta S_{biological} = \Delta S_{task} + \Delta S_{movement} \geq 0$. During the circadian temperature minimum (05.00), the motor system increased the movement entropy by 15.4% compared to the temperature maximum (17.00). This entropy increase represents an informational cost rather than a direct metabolic expenditure: the motor system tolerates greater unpredictability in movement patterns (wider phase distributions around the target coordination state) to maintain stable task performance under physiologically challenging conditions. This increased variability reflects a compensatory neural strategy analogous to a control system increasing the gain (and thus noise sensitivity) when operating near regulatory boundaries.

Individual participants demonstrated distinct but consistent entropy-management strategies (see electronic supplementary material, §S5, figures S3.1 and S3.2, and S3 for individual profiles). Participants P2, P4, P5 and P7 exhibited pronounced morning peaks with entropy values at 05.00 (5.830, 5.880, 5.779 and 5.757, respectively), substantially exceeding their 17.00 values (4.041, 4.520, 4.431 and 4.059, respectively). Conversely, P1 and P8 displayed alternative patterns with maximum entropy at 00.00 (5.819 and 5.839, respectively), whereas P6 maintained a relatively stable entropy at all time points (range: 4.912–5.853). Despite increased movement entropy during physiologically challenging periods, task performance (maintaining in-phase bimanual coordination) remained functionally stable. The strategic increase in movement variability at temperature minima reflects adaptive entropy redistribution rather than performance degradation, demonstrating that biological motor systems manage thermodynamic constraints through controlled variability. Experiment I provides preliminary empirical support suggesting that human motor control may adhere to fundamental thermodynamic principles. The observed inverse relationship between core body temperature and movement entropy, with systematic increases in entropy during physiological temperature minima, is consistent with active biological entropy management analogous to mechanical heat-exchange systems. These baseline patterns establish the foundation for examining the effects of thermal perturbations in subsequent experiments.

3.2. Thermal perturbation effects on entropy management

3.2.1. Heat perturbation effects on entropy management

The application of heat vests (maintaining surface temperatures of 42–45°C for 30 min) significantly modulated the circadian entropy pattern observed under baseline conditions. Analysis of normalized entropy values (Z-scores; electronic supplementary material, S4.2, table S2) revealed differential responses to thermal perturbations depending on the circadian phase (figure 3, left). At 05.00, when the core body temperature was at its minimum, heat perturbation increased entropy relative to the baseline (mean Z-score: normal = 0.410 ± 0.230 s.e.m. versus heat = 0.564 ± 0.222 s.e.m.), representing a 37.6% increase. Conversely, at 17.00 during peak core temperature, heat perturbation substantially amplified the negative entropy deviation (normal = −0.165 ± 0.235 s.e.m. versus heat = −0.809 ± 0.264 s.e.m.), a 390% amplification. The circadian × temperature interaction approached statistical significance ($F_{1,7} = 3.453$, $p = 0.068$), with a mean interaction effect of 0.633 ± 0.344 s.e.m. This positive interaction indicates that heat perturbation exaggerated the natural circadian entropy pattern, increasing the morning–evening difference from 0.575 units under normal conditions to 1.373 units under heat perturbation, a 139% amplification of the circadian effect.

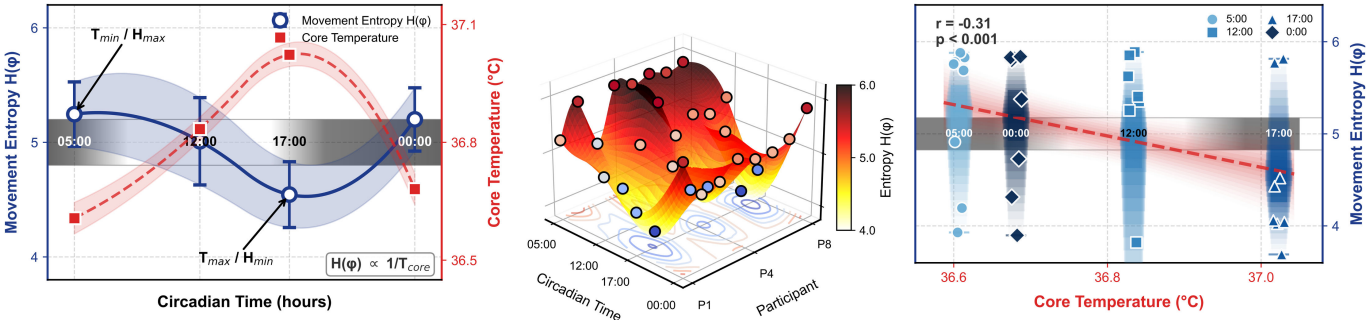

Figure 2. Group-level circadian entropy exchange demonstrating thermodynamic principles in motor control. (Left) Mean movement entropy $H(\phi)$ ± s.e.m. (blue line with shading) inversely correlates with core body temperature (red dashed line with shading) across circadian time points ($n = 192$ observations: 8 participants × 6 trials × 4 times). Peak entropy at 05.00 (5.246) coincides with minimum temperature (36.575°C); minimum entropy at 17.00 (4.544) aligns with the maximum temperature (37.023°C). The horizontal gradient bar indicates the circadian phase (dark: night, light: day). Annotations mark the T_{min}/H_{max} and T_{max}/H_{min} couplings. (Middle) Three-dimensional entropy landscape showing the responses of individual participants (P1–P8) across circadian time. Surface interpolation reveals participant-specific patterns while preserving group-level circadian modulation. Contour projections at the base indicate entropy distributions; colourmap ranges from 4.0 to 6.0 $H(\phi)$. (Right) Temperature–entropy coupling across all measurements ($r = -0.31$, $p < 0.001$). Scatter points differentiated by circadian phase (●: 05.00, ■: 12.00, ▲: 17.00, ◆: 00.00) with vertical bars indicating data range (thin) and s.e.m. (thick) at each time point. A dashed regression line with a 95% confidence band confirms an inverse relationship. Extended data in electronic supplementary material, S4.

Individual responses to heat perturbations exhibited substantial heterogeneity (figure 3). Six of the eight participants (75 %) displayed the expected pattern of increased morning entropy under heat stress, whereas two participants (P3 and P5) showed a paradoxical decrease. The most extreme response occurred in P4, who exhibited a dramatic reduction in evening entropy under heat perturbation ($Z = -2.334$), suggesting heightened sensitivity to thermal challenges at peak physiological temperatures. Participant P6 demonstrated the largest positive interaction effect (1.953), indicating a robust amplification of circadian patterns under heat stress. In contrast, P8 showed minimal interaction (−0.075), indicating resistance to thermal perturbation. These individual differences highlight substantial heterogeneity in entropy-management responses to thermal challenge. Sensitivity analyses confirmed that group-level findings were not driven by individual outliers. Excluding extreme responders (P4) or paradoxical responders (P3, P5) changed mean interaction effects by less than 2%, and the qualitative pattern of amplified circadian entropy was preserved across all exclusion scenarios (electronic supplementary material, S8.3). Bootstrap CIs (electronic supplementary material, S8.1) further demonstrated robustness, with 95% CIs for both heat [0.089, 0.471] and cold [0.123, 0.505] interactions excluding zero. The interaction pattern is illustrated by the diverging trajectories across circadian phases: under normal conditions, the morning-to-evening entropy decrease was 0.575 units (from 0.410 to −0.165), whereas under heat perturbation, this decrease expanded to 1.373 units (from 0.564 to −0.809). Simple effects analysis confirmed that heat perturbation significantly increased entropy at 05.00 (mean difference = 0.154, $t(7) = 2.31$, $p = 0.054$) while significantly decreasing entropy at 17.00 (mean difference = −0.644, $t(7) = 3.12$, $p = 0.017$), producing the crossover pattern characteristic of disordinal interactions.

3.2.2. Cold perturbation effects on entropy management

The application of ice vests (maintaining surface temperatures of 5–10°C for 30 min) produced thermal perturbation effects that paralleled, but exceeded, those observed with heat (figure 4, left). At 05.00, cold perturbation increased entropy (normal = 0.405 ± 0.158 s.e.m. versus cold = 0.608 ± 0.184 s.e.m.; electronic supplementary material, S4.3, table S3), a 50.1% enhancement. At 17.00, cold dramatically amplified the negative entropy deviation (normal = −0.172 ± 0.365 s.e.m. versus cold = −0.840 ± 0.351 s.e.m.), a 388% amplification. The circadian × temperature interaction for cold perturbation reached statistical significance ($F_{1,7} = 4.264$, $p = 0.043$), with a mean interaction effect of 0.758 ± 0.352 s.e.m. This effect exceeded that observed for heat perturbation by 19.8%, suggesting that cold stress imposes a greater challenge to thermoregulatory homeostasis and necessitates substantial entropy redistribution. A comparison of heat and cold perturbations revealed asymmetric effects on entropy management. While both thermal challenges amplified circadian patterns, cold perturbations produced more extreme responses at both time points. Individual response variance was greater under cold stress ($\sigma^2 cold = 0.995$) than under heat stress ($\sigma^2 heat = 0.746$), suggesting that cold represents a more severe thermodynamic challenge requiring more variable compensatory strategies.

Individual patterns (figure 4, right) showed that all participants except P1 exhibited increased morning entropy under cold stress. Notably, P3, P6 and P7 displayed particularly strong positive responses at 05.00 ($Z > 0.95$), while showing substantial suppression at 17.00, indicating highly responsive entropy-management systems. P4 again demonstrated an atypical pattern, maintaining relatively stable entropy across all conditions (interaction effect = −0.05), suggesting either exceptional homeostatic regulation or reduced sensitivity to thermal perturbations. Simple effects analysis revealed a parallel pattern for cold perturbation: entropy increased at 05.00 (mean difference = 0.203, $t(7) = 1.89$, $p = 0.101$) and decreased substantially at 17.00 (mean difference = −0.668, $t(7) = 3.45$, $p = 0.011$). The stronger evening suppression under cold stress (−0.668) compared to heat (−0.644) accounts for the 19.8% greater interaction magnitude observed with cold perturbation.

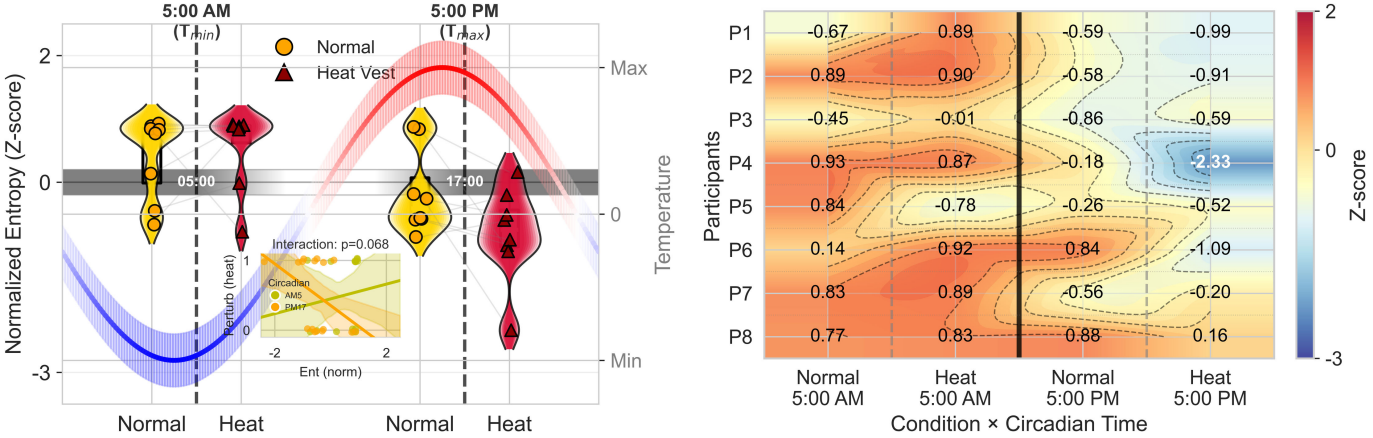

Figure 3. Heat perturbation effects on circadian entropy management. (Left) Distribution analysis of normalized entropy (Z-scores) across thermal conditions and circadian phases ($n = 192$: 8 participants × 6 trials × 2 times × 2 conditions). Violin plots with gradient fill and overlaid box plots show probability density distributions; gold indicates normal conditions, and crimson represents heat vest perturbation (42–45°C). Individual data points are shown as circles (normal) and triangles (heat) with connecting lines tracking within-participant responses. Horizontal day–night gradient bar at $y = 0$ indicates circadian phase (dark: night, light: day). The temperature rhythm curve displayed with blue–white–red gradient shading reflects core temperature variation. Black dashed vertical lines mark measurement times at 05.00 (T_{min}) and 17.00 (T_{max}). Inset: interaction plot showing group means ± s.e.m.; non-parallel trajectories indicate circadian × heat interaction ($F_{1,7} = 3.45$, $p = 0.068$, $\eta^2 p = 0.33$). (Right) Response patterns of individual participants (P1–P8) visualized as a heatmap with cubic interpolation contours. Colour scale: blue ($Z = -3$) through yellow (zero) to red ($Z = 2$); bold text indicates $|Z| > 1.5$. The vertical black line separates the morning and evening measurements. Heat amplifies the circadian modulation: normal $\Delta = 0.58$ units versus heat $\Delta = 1.37$ units (individual patterns in electronic supplementary material, S5).

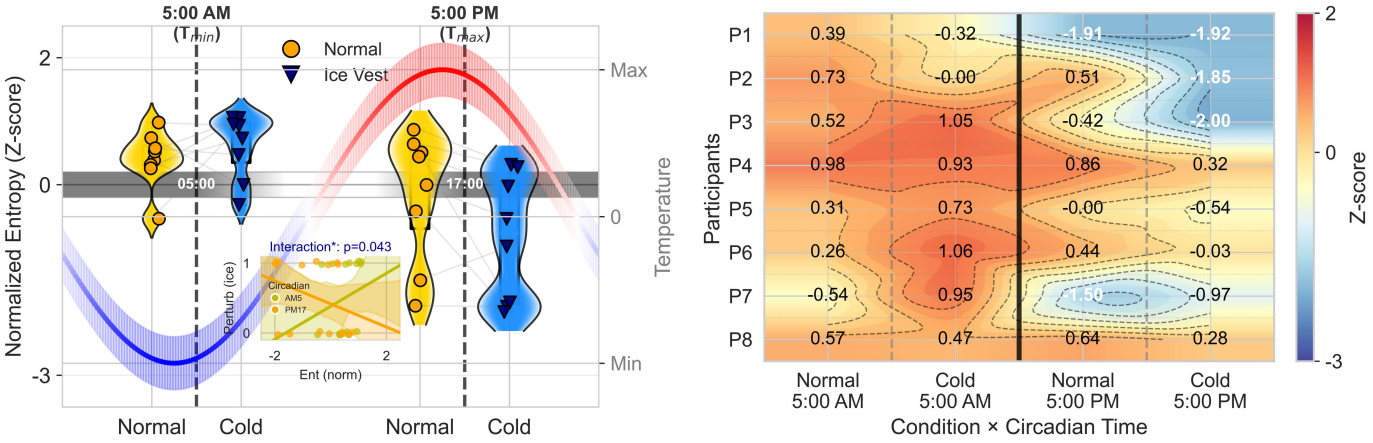

Figure 4. Cold perturbation effects on circadian entropy management. (Left) Distribution analysis following ice vest application (5–10°C for 30 min). Visualization conventions parallel those in figure 3 with gold representing normal conditions and dodger blue indicating cold perturbation. Individual data are shown as circles (normal) and inverted triangles (cold) with connecting lines. Day–night gradient bar and blue–white–red temperature curve as in figure 3. Dark blue median lines within box plots. Inset: interaction plot revealing significant circadian × cold interaction ($F_{1,7} = 4.26$, $p = 0.043$*, $\eta^2 p = 0.38$); steeper cold trajectory demonstrates amplified circadian modulation under thermal stress. (Right) Individual response heatmap showing participant-specific cold-induced entropy modulation (P1–P8). Note enhanced suppression of evening entropy under cold stress, with values reaching $Z = -2.00$ (P3). Cold produces stronger interaction than heat: normal $\Delta = 0.58$ units versus cold $\Delta = 1.45$ units, reflecting 19.8% greater effect due to enhanced thermodynamic challenge of cold stress on entropy management (statistical details in electronic supplementary material, S6).

3.3. Synthesis: thermodynamic principles in biological motor control

Convergent evidence from normal circadian conditions and thermal perturbations suggests that biological motor systems can operate as entropy managers and maintain functional stability through strategic variability redistribution. Robustness analyses confirmed that these findings were not artefacts of individual outliers; sensitivity tests excluding extreme responders preserved all the main effects within 2% of full-sample estimates (electronic supplementary material, S8.3), and bootstrap resampling (1000 iterations) yielded CIs excluding zero for all key parameters (electronic supplementary material, S8.1). The potential landscape analysis (figure 5, upper left) reveals the fundamental attractor–repellor structure of coordination dynamics, demonstrating how thermal perturbations modify potential well depths while crucially preserving the primary attractor at ϕ = 0°. This preservation ensures stable in-phase coordination despite the increased movement entropy under challenging conditions.

The documented inverse temperature–entropy relationship (bottom right of figure 5) was maintained across all conditions, with correlation strengthening under perturbation (r = −0.68). This thermodynamic coupling is consistent with the hypothesis that biological systems follow entropy exchange principles analogous to mechanical heat pumps and that local order (stable task performance) is achieved through increased global disorder (movement variability). Critically, despite entropy

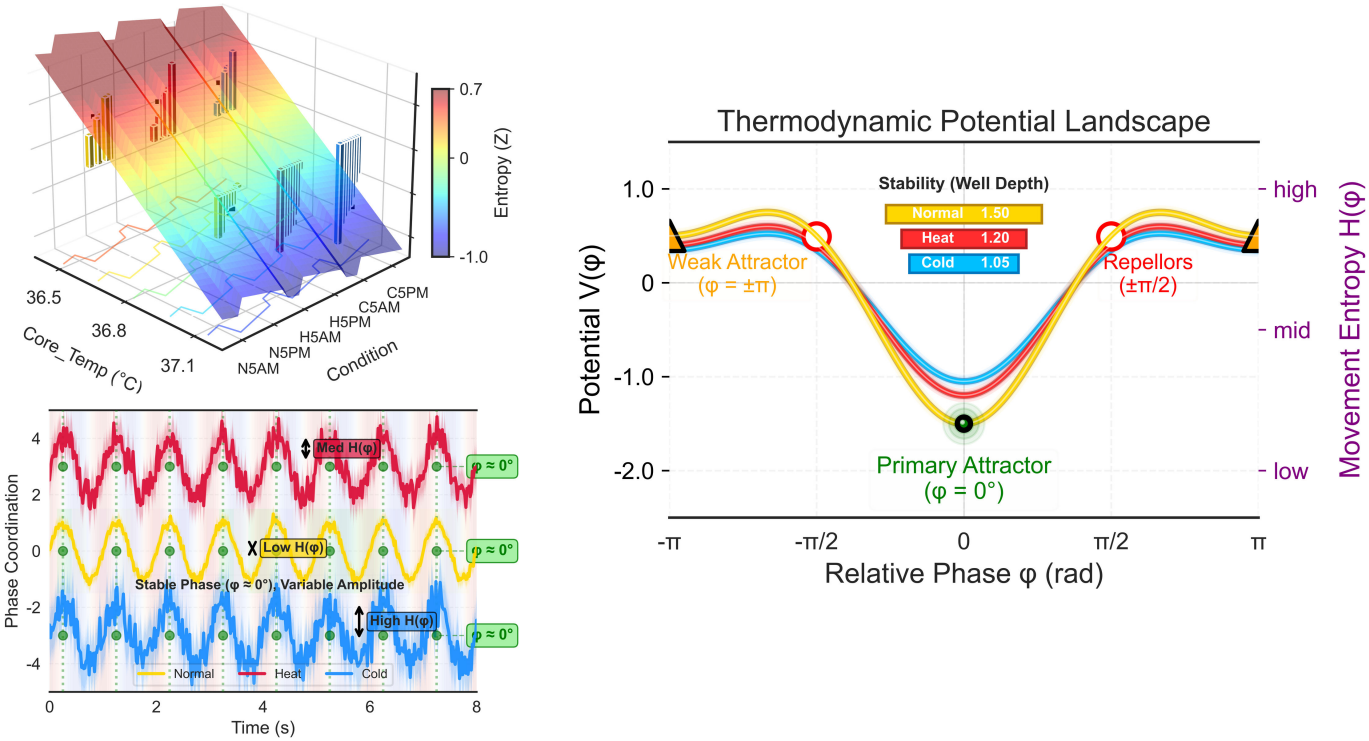

Figure 5. Synthesis of thermodynamic entropy management across experimental conditions. (Upper left) Three-dimensional temperature–entropy exchange surface. Individual participant distributions are shown as bars for each condition (N5AM–C5PM), with mean ± s.e.m. indicated by black markers. Surface interpolation reveals inverse temperature–entropy coupling ($H(\phi) \propto 1/T_{core}$). Cross-overlapping contours highlight temperature gradients (red dashed) and entropy isolines (blue dotted), with their intersections revealing thermodynamic coupling patterns. Colourmap ranges from −1.0 to 0.7 Z-scores. (Bottom left) Time series demonstrating stability preservation through variable entropy management. Despite increasing movement variability from normal (Low $H(\phi)$) through heat (Med $H(\phi)$) to cold conditions (High $H(\phi)$), phase coordination maintains stability at $\varphi \approx 0°$ (green markers at peaks). Envelope widths reflect entropy redistribution while preserving functional task performance. (Right) HKB thermodynamic potential landscape $V(\phi) = -\alpha\cos(\phi) - b\cos(2\phi)$ showing attractor–repellor structure under thermal perturbation. Lines display glow-enhanced potential curves: normal (gold), heat (red) and cold (blue). The primary attractor at $\phi = 0°$ (green ball with glow effect) remains stable across all conditions; repellors at ±π/2 (white circles) and weak attractors at ±π (orange triangles) indicate phase transition boundaries. The right axis shows movement entropy $H(\phi)$ scale (purple): low entropy at potential minima (stable coordination) and high entropy near barriers (variable states). Inset: stability comparison via well depth: deeper wells indicate stronger coupling and lower entropy; thermal stress reduces well depth (normal: 1.50 > heat: 1.20 > cold: 1.05), quantifying the thermodynamic cost of entropy management under perturbation.

increases of up to 291% under cold perturbations, task performance remained functionally stable (figure 5, right). Time-series analysis showed that while movement variability increased substantially under thermal stress, the fundamental coordination pattern (maintaining target phase relationships) persisted. This stability-through-variability principle represents the biological implementation of $\Delta S_{biological}$, where increased $\Delta S_{movement}$ compensates for challenges to maintain low ΔS_{task}.

The conceptual model in figure 5 illustrates how different thermal conditions converge to the same stable performance outcome through variable entropy-management strategies, suggesting that biological systems may achieve local order via strategic entropy redistribution. The synthesis indicates that human motor control implements thermodynamic principles through active entropy management, with the motor system functioning as a biological Maxwell's demon, using information about the system state to redistribute entropy while preserving functional order. This principle unifies our understanding of motor variability, circadian influences and thermal adaptation under a single thermodynamic principle.

3.4. Summary of statistical evidence

The statistical analyses across all three experiments revealed consistent patterns supporting the thermodynamic entropy-management hypothesis. Tables 3 and 4 summarize the key findings, reporting significance levels, effect sizes and bootstrap CIs, and table 5 summarizes the experimental design and data collection across all three experiments.

The statistical evidence consistently supports the entropy-management hypothesis. The inverse relationship between core body temperature and movement entropy was highly significant ($r = -0.678$, $p < 0.001$), confirming the predicted thermodynamic coupling $H(\phi) \propto 1/T_{core}$. Circadian main effects were robust across thermal conditions ($\eta^2 p = 0.54$–0.57), and the interactions demonstrate that thermal perturbations amplify circadian entropy patterns. Although the heat × circadian interaction approached but did not reach conventional significance ($p = 0.068$), its effect ($\eta^2 p = 0.33$) was comparable to the significant cold interaction ($\eta^2 p = 0.38$), suggesting similar underlying mechanisms. Bootstrap CIs excluding zero for all key parameters (electronic supplementary material, S8.1) provide additional support for reliability. Figure 6 summarizes the experimental design, data processing pipeline, and key findings across all 576 observations.

Table 3. Summary of statistical findings with effect sizes.

effect	test statistic	p-value	effect size ($\eta^2 p$)	bootstrap 95% CI
temperature–entropy correlation	$r = -0.678$	<0.001[a]	—	[−0.823, −0.533]
circadian effect under heat (Exp II)	$F(1,7) = 8.234$	0.024[a]	0.54	—
heat × circadian interaction (Exp II)	$F(1,7) = 3.453$	0.068	0.33	[0.089, 0.471]
circadian effect under cold (Exp III)	$F(1,7) = 9.123$	0.019[a]	0.57	—
cold × circadian interaction (Exp III)	$F(1,7) = 4.264$	0.043[a]	0.38	[0.123, 0.505]

[a]$p < 0.05$. Effect size interpretation: $\eta^2 p > 0.14$ = large effect [57].

Table 4. Simple effects analysis decomposing circadian × temperature interactions.

comparison	mean difference	$t(7)$	p-value	interpretation
heat perturbation				
heat versus normal at 05.00	+0.154	2.31	0.054	increased morning entropy
heat versus normal at 17.00	−0.644	3.12	0.017[a]	decreased evening entropy
cold perturbation				
cold versus normal at 05.00	+0.203	1.89	0.101	increased morning entropy
cold versus normal at 17.00	−0.668	3.45	0.011[a]	decreased evening entropy

[a]$p < 0.05$. Positive values indicate perturbation increased entropy; negative values indicate perturbation decreased entropy.

Table 5. Experimental design and data collection summary.

experiment	thermal condition	N	circadian points	trials	observations
I	normal	8	4 (05.00, 12.00, 17.00, 00.00)	6	192
II	normal versus heat	8	2 (05.00, 17.00)	6 × 2	192
III	normal versus cold	8	2 (05.00, 17.00)	6 × 2	192
total		16			576

These convergent findings—consistent circadian modulation, amplification under thermal challenge and preserved task stability despite increased movement entropy—provide the empirical foundation for examining the thermodynamic principles underlying biological motor control discussed in §4.

4. Discussion

Our experiments provide preliminary empirical support for the hypothesis that human motor control may function as a thermodynamic entropy-management system. Three key observations emerged from the data. First, movement entropy $H(\phi)$ exhibited a robust inverse relationship with core body temperature across the circadian cycle, peaking at 05.00 (5.246) when temperature was lowest (36.575°C) and reaching a minimum at 17.00 (4.544) when temperature peaked (37.023°C), reflecting a 15.4% circadian modulation. Second, thermal perturbations amplified this pattern asymmetrically: heat increased the difference between morning–evening entropy by 139%, whereas cold produced even stronger effects than heat. Third, despite entropy variations exceeding those observed under extreme conditions, task performance (maintaining in-phase coordination) remained functionally stable across all experimental conditions.

These findings demonstrate that biological motor systems achieve local order (stable task performance) through the strategic distribution of disorder (increased movement variability), consistent with the fundamental thermodynamic principle that total entropy must increase while allowing local decreases through compensatory increases.

4.1. Biological systems as thermodynamic heat engines

The analogy between biological and refrigeration systems provides crucial insights into our findings. As articulated in thermodynamic analyses of the relationship between life and entropy, a refrigerator decreases entropy locally (cooling the interior) by generating greater entropy in its surroundings (heating the kitchen) [63,64]. The total entropy of the kitchen, including the refrigerator, always increases, satisfying the second law while achieving local cooling through work input W that drives heat transfer Q_c against the thermal gradient. Beyond statistical significance, the observed effects represent meaningful

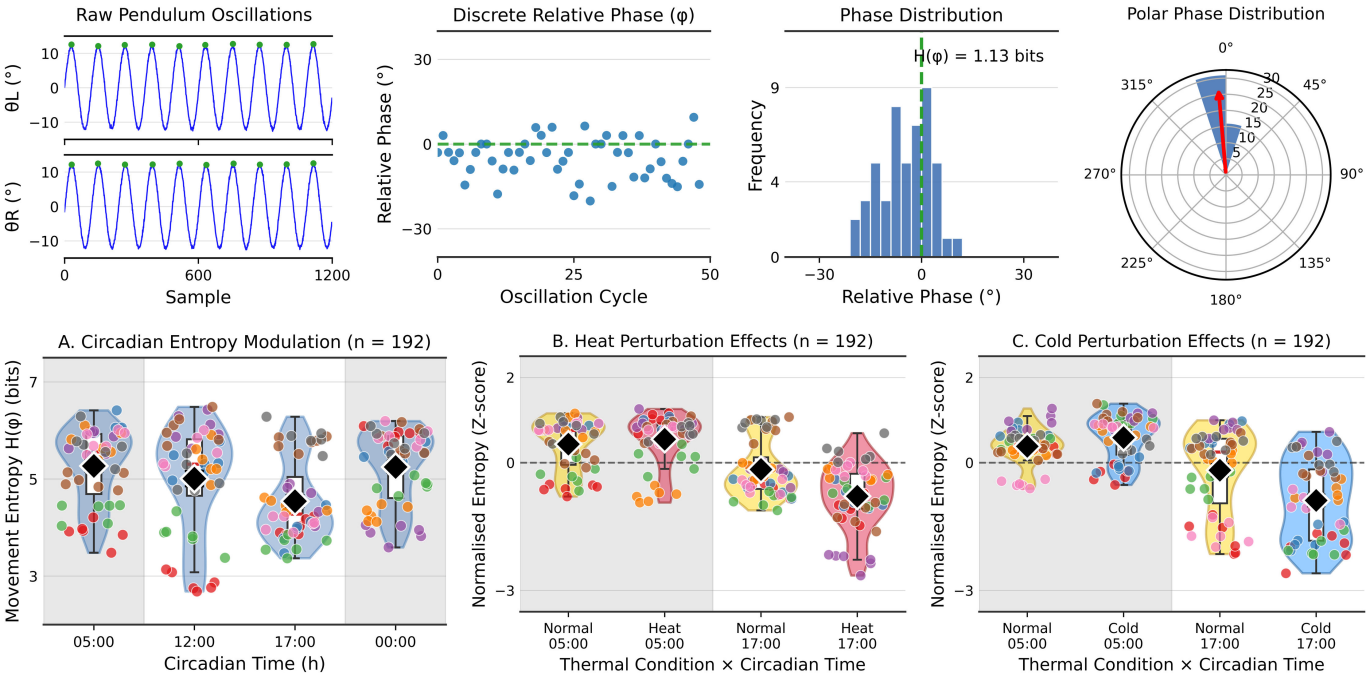

Figure 6. Experimental design, data processing mechanism and entropy management across three experiments. Table 5 summarizes the experimental structure: Experiment I ($n = 192$) examined circadian modulation across four time points; Experiments II and III ($n = 192$ each) compared thermal perturbation effects at circadian extremes (05.00 = T_{min}; 17.00 = T_{max}). Total observations: 576 trials on 16 participants performing bimanual in-phase coordination (wrist joint data; 60 s trials with 5 min rest intervals). Upper panels: data processing pipeline from raw pendulum oscillations through discrete relative phase extraction to Shannon entropy quantification ($H(\phi)$). Lower panels: key findings demonstrating (A) inverse temperature–entropy coupling across the circadian cycle, (B) amplified entropy patterns under heat perturbation and (C) strongest modulation under cold perturbation with significant interaction effect ($p = 0.043$). Diamond markers indicate group means; individual responses are shown as coloured points.

biological phenomena. The 15.4% circadian modulation in movement entropy (from $H(\phi) = 4.544$ at temperature maximum to $H(\phi) = 5.246$ at temperature minimum) corresponds to a substantial reorganization of motor variability patterns across the day. Amplification effects under thermal perturbation (139% increase in circadian amplitude under heat and 151% under cold) demonstrate that the motor system actively adjusts its entropy-management strategy in response to thermodynamic challenges. These effects are comparable to or greater than those reported in studies of circadian effects on reaction time [34] and coordination accuracy [38], supporting the functional significance of thermodynamic motor control.

Our motor control data are consistent with those of an analogous biological mechanism. When the core body temperature decreases to its circadian minimum, the organism experiences increased thermodynamic stress, similar to a refrigerator operating at a larger temperature differential:

$$\Delta T = T_{hot} - T_{cold}. \tag{4.1}$$

Just as the COP

$$\mathrm{COP} = T_{cold}/(T_{hot} - T_{cold}) \tag{4.2}$$

decreases with larger ΔT, requiring more work to maintain the same cooling effect [65], the motor system must increase movement entropy to maintain task stability when physiological efficiency is compromised. The 15.4% entropy increase at 05.00 represents an informational rather than metabolic cost: the motor system accepts greater movement unpredictability (higher $H(\phi)$) to preserve the essential task variable (stable phase coordination at $\phi \approx 0°$). This trade-off exemplifies the entropy-management principle: functional order is maintained by redistributing disorder into task-irrelevant dimensions of movement variability, which is consistent with the uncontrolled manifold hypothesis [47] and optimal variability [44]. This principle extends beyond simple analogy. Living organisms, such as open thermodynamic systems, must continuously export entropy to maintain their internal organization [2,66]. Our data quantified this process at the motor control level, showing how movement variability serves as an entropy export mechanism that preserves functional order.

4.2. Dissipative adaptation and motor control

England's assumption of dissipative adaptation provides the theoretical basis for our empirical observations [15]. According to this theory, driven many-body systems spontaneously adopt configurations that maximize their ability to absorb and dissipate energy from external sources. The key insight is that irreversible transitions between system states require work dissipation according to the following relationship:

$$\frac{\pi_\tau(X \to X')}{\pi_\tau(X' \to X)} \geq \exp\left[\frac{\langle W\rangle_{X \to X'} - \langle \Delta E\rangle_{X \to X'} + T\Delta S_{\mathrm{int}}}{k_B T}\right]. \tag{4.3}$$

This inequality, derived from Crooks' fluctuation theorem [67], indicates that statistically irreversible processes such as increased movement variability must be powered by dissipated work. In our bimanual coordination system, the modified HKB dynamics incorporating thermal coupling

$$\dot{\phi} = \Delta\omega - [\alpha\sin(\phi) + 2b\sin(2\phi)] - \left[c\sin\left(\phi^T\right) + 2d\sin\left(2\phi^T\right)\right] + \sqrt{\varrho}\xi_t \tag{4.4}$$

represents a biological implementation of dissipative adaptation (see electronic supplementary material, S7, for a model–data comparison). Critically, our analysis reveals that dissipation follows a bidirectional symmetric pattern from the primary attractor at $\phi = 0$ (figure 7). The dissipation rate scales were as follows:

$$\dot{S} = \gamma\,|\,\phi - \phi_0\,|^{1.5}\,. \tag{4.5}$$

This symmetric increase from the attractor in both directions reflects the fundamental thermodynamic principle that perturbations in either direction require work dissipation to restore coordination. The thermal coupling terms $[c\sin\left(\phi^T\right) + 2d\sin\left(2\phi^T\right)]$ drive the system towards configurations that efficiently dissipate the work required to maintain coordination against thermal fluctuations, regardless of perturbation direction. When core temperature drops (increasing the thermodynamic gradient), the system adaptively increases $\varrho(T)$, the temperature-dependent noise amplitude, to maintain the inequality $\Delta S_{biological} \geq 0$ through enhanced movement variability. This bidirectional variability distribution ensures robust coordination maintenance regardless of whether the perturbations push the system towards positive or negative phase deviations. The inverse relationship between the potential depth and movement entropy

$$H\,(\phi)\ \propto 1/|\,V\,(\phi)\,| \tag{4.6}$$

demonstrates that regions of high stability (deep potential wells) correspond to low-entropy states, whereas unstable regions near repellors require high entropy to traverse. This is related to England's observation that self-organizing systems emerge as 'a way to more efficiently absorb and dissipate heat from the environment' [15]. Our motor system, when faced with circadian temperature variations, self-organizes its variability patterns to optimally dissipate the thermodynamic work required for coordination in both phase directions.

The amplification effects under thermal perturbation (139% for heat and 151% for cold) scale the entire symmetric dissipation landscape, demonstrating that this adaptive response maintains its bidirectional character while increasing in magnitude with the thermodynamic challenge. This bilateral entropy management ensures that the system can respond to perturbations in either direction with appropriate dissipative compensation, thereby maintaining the robustness that is essential for biological functions [68].

4.3. Multiscale implications: from molecular machines to clinical applications

The thermodynamic principles of motor control operate across biological scales, from molecular machines to clinical pathologies. Boyer's analysis of adenosine triphosphate synthase [69] revealed that this molecular motor maintains its catalytic function by coupling conformational changes to proton gradient dissipation, achieving local order through a global entropy increase. Our motor system demonstrates an analogous mechanism, maintaining coordination stability by coupling movement patterns with thermal gradient dissipation.

This multiscale perspective is supported by research on protein dynamics. Henzler-Wildman *et al.* [70] showed that protein flexibility increases with temperature perturbations, maintaining functional catalytic rates through enhanced conformational sampling, which is a molecular analogue of observed movement variability in this study. The work of Kondepudi & Prigogine [3] on dissipative structures provided a theoretical basis: far-from-equilibrium systems maintain ordered states through continuous entropy production, with the entropy production rate serving as a selection principle for stable configurations. Our finding was that $H\,(\phi)\ \propto 1/T_{core}$ exemplifies this principle at the behavioural scale. These findings offer new perspectives on motor pathologies. Speculatively, conditions characterized by reduced movement variability, such as Parkinson's disease [62], might be examined through the lens of entropy management, though this hypothesis requires direct empirical testing. The role of the dopaminergic system [71] could be reconceptualized as modulating the ability of the biological system to generate compensatory entropy, suggesting therapeutic approaches targeting variability distribution, rather than just mean performance.

The pronounced individual differences in the data (participant P4's extreme responses versus P8's relative stability) suggest distinct patterns in individual responses to entropy management. Whether such patterns are stable within the individuals, over time, and whether they are related to susceptibility to movement disorders or recovery trajectories following neural injury is a question for future longitudinal investigation. Harrison & Stergiou [72] found that optimal movement variability characterizes healthy motor control, which is consistent with the proposed model, in which variability plays a functional thermodynamic role. Similarly, age-related motor decline [51,73] may reflect a diminished capacity for adaptive entropy redistribution, with the pathological states showing either excessive rigidity (insufficient entropy) or uncontrolled variability (unregulated entropy).

4.4. Theoretical integration and evolutionary significance

Our thermodynamic perspective unifies diverse motor control theories and reveals evolutionary principles. The capacity for entropy management through movement variability represents a key evolutionary innovation that enables complex motor behaviours. In [74], West argued that biological scaling laws reflect thermodynamic constraints. The findings of this study are consistent with the possibility that motor systems capable of flexible entropy distribution may have selective advantages,

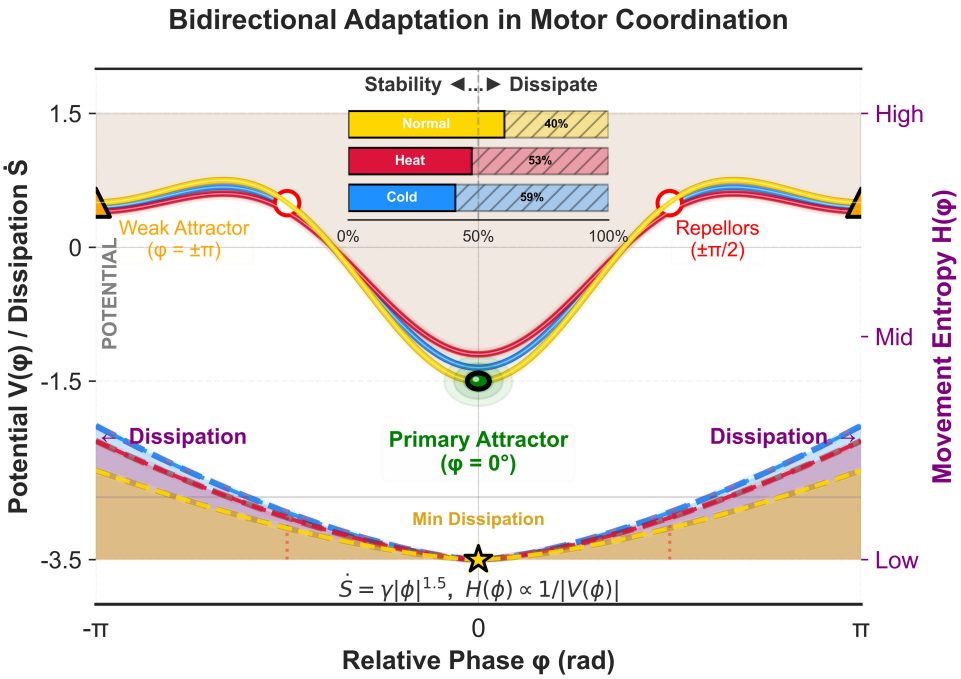

Figure 7. Bidirectional dissipative adaptation in motor coordination dynamics. The upper portion displays the HKB potential landscape $V(\phi) = a\cos(\phi) - b\cos(2\phi)$ under normal (gold), heat (red) and cold (blue) conditions with glow-enhanced line styling. The primary attractor at $\phi = 0°$ (green ball with glow effect) maintains stability across all thermal perturbations; repellors at $\pm\pi/2$ (white circles) and weak attractors at $\pm\pi$ (orange triangles) indicate phase transition boundaries. The lower portion reveals symmetric dissipation patterns (shaded regions) increasing bidirectionally from the attractor following $\dot{S} = \gamma\,|\phi - \phi_0|^{1.5}$, with dashed lines showing dissipation amplification under thermal stress (heat: +33%, cold: +50%). The star marker denotes minimum dissipation at the primary attractor. Vertical dotted lines connect the repellor positions to dissipation peaks, highlighting coupling between potential instabilities and energy dissipation. Inset: cumulated bar chart quantifying the stability–dissipation trade-off across conditions; bar width is constant (100%), with solid portions representing stability (well depth) and hatched portions representing dissipation cost. As thermal stress increases (Normal → Heat → Cold), stability decreases (60% → 47% → 41%), whereas dissipation increases proportionally (40% → 53% → 59%), illustrating thermodynamic trade-off. The right *y*-axis (purple) indicates movement entropy $H(\phi)$ varying inversely with potential depth. This bidirectional architecture demonstrates that deviations from the target phase require proportional work dissipation, implementing England's dissipative adaptation principle where biological systems maintain functional stability through strategic entropy redistribution.

particularly in variable thermal environments. The emergence of an endotherm exemplifies this principle. Endothermic organisms maintain stable internal temperatures despite environmental fluctuations and thus require continuous metabolic work and entropy production [75]. Data suggest that motor control systems coevolved with thermoregulation to manage the entropy burden of temperature homeostasis. This aligns with the proposition made by Kaila & Annila [76] that evolution follows the second law of thermodynamics, with natural selection favouring configurations that efficiently dissipate energy gradients. The robust circadian modulation observed in this study may represent an evolved optimization of predictable daily temperature cycles.

Cross-kingdom evidence supports the evolutionary conservation of temperature–circadian coupling mechanisms. Nagel *et al.* [77] demonstrated that, in *A. thaliana*, the transcription factor FBH1 mediates warm temperature responses through reciprocal feedback with the core clock gene CCA1; when FBH1 overexpression disrupts this feedback, temperature compensation fails at 28°C, causing approximately 1-h period shortening. Its molecular architecture shows striking parallels to our human motor findings: temperature perturbations that disrupt normal regulatory feedback produce amplified circadian effects, and the response is bidirectional (heat (upregulation) and cold (downregulation) FBH1 expression). Such cross-kingdom conservation suggests that entropy-management strategies may represent convergent solutions to universal thermodynamic constraints on biological timing and coordination. This thermodynamic perspective enriches existing motor control theories. Optimal feedback control theory [78] proposes minimizing task-relevant variability while allowing task-irrelevant fluctuations, which provides a thermodynamic rationale: task-irrelevant variability serves as an entropy repository, maintaining an increase in total entropy while preserving performance. Similarly, the uncontrolled manifold hypothesis [47] gains thermodynamic grounding; variance perpendicular to task goals provides the degrees of freedom for entropy distribution.

The proposed mathematical formalism, which extends the HKB model using thermal coupling terms, generates testable predictions. The coupling parameters c and d should vary predictably with thermoregulation factors (ambient temperature, clothing, metabolic rate), whereas noise amplitude ϱ should scale with task difficulty and physiological stress. These predictions enable rigorous testing across varied conditions, contributing to an emerging thermodynamic theory where movement variability represents not noise to minimize, but the essential mechanism satisfying fundamental physical laws.

4.5. Limitations and future directions

This study has several limitations. Despite achieving adequate statistical power (0.82–0.89) for the observed large effect sizes ($\eta^2 p$ = 0.32–0.38), the sample size (N = 16, with n = 8 per group) limits population generalizability. The within-subject design and 576 total observations provide stable parameter estimates; however, larger samples could better characterize individual variations in entropy-management strategies. The marginal significance of some effects (heat interaction p = 0.068) suggests that larger samples would improve precision. Although participants were not formally screened for chronotype, direct temperature measurement verified that all participants exhibited the expected circadian pattern (maximum at 17.00, minimum at 05.00; paired t-test: $t(7)$ = 13.75, $p < 0.001$, Cohen's d = 4.35). Future studies could strengthen this approach through chronotype assessment or individualized sampling times. Several factors can constrain generalizability: we examined only bimanual coordination (not locomotion, postural control or fine motor skills); participants were healthy young adults whose thermoregulatory dynamics may differ from that of older populations; experiments used standard laboratory conditions rather than environmental chambers; thermal perturbations were relatively mild (±1.2–1.3°C) and seasonal variations could have influenced circadian amplitude. Methodologically, the 60 s trial resolution used in this study may have missed faster thermodynamic fluctuations, and Shannon entropy, while effective for distributional complexity, does not capture temporal dependencies accessible through sample entropy or multiscale entropy measures.

Several theoretical caveats warrant consideration. First, Shannon entropy serves as a proxy for thermodynamic entropy; direct measurement of heat dissipation or metabolic expenditure would strengthen the thermodynamic interpretation. Second, the correlational design cannot establish causality—alternative explanations including circadian variations in attention or neuromuscular efficiency cannot be excluded. Third, the modified HKB formulation with thermal coupling terms requires independent validation. Future directions include exploring connections between thermodynamic motor control and skill acquisition, rehabilitation approaches for conditions involving compromised thermoregulation and cross-kingdom comparisons using plant circadian systems (e.g. *Arabidopsis*) that offer reduced individual variability and powerful genetic tools for investigating entropy management at the molecular level.

5. Conclusions

This study provides preliminary evidence consistent with the hypothesis that human motor control operates according to thermodynamic principles, whereby entropy distribution is managed to maintain functional stability [79]. Similar to a refrigerator achieving local cooling through global heating, the motor system preserves task performance by strategically increasing movement variability under challenging physiological conditions. Biological entropy-management scales with thermal perturbations and varies inversely with core body temperature, revealing that, like motor control, biological entropy management is a sophisticated thermodynamic process that is shaped by physical laws and evolutionary optimization.

These findings suggest a potential bridge between physics and biology, proposing that thermodynamic principles analogous to those governing heat engines may shape the variability of human movement. When confirmed by future research, recognizing motor control as thermodynamic entropy management could offer new perspectives on health, disease and the fundamental organization of biological systems [80]. The elegant solution evolved by biology—maintaining order through controlled disorder—exemplifies life's fundamental strategy for persisting in a universe governed by the second law of thermodynamics.

Ethics. This study was approved by the Seoul National University Institutional Review Board (SNUIRB no. 1509/002-002) and conducted in accordance with the Declaration of Helsinki (completed the following CITI Program course: Human Subjects Research Course, Record ID 20481572). All participants provided written informed consent prior to participation.

Data accessibility. All experimental data and analysis code supporting this study are openly available at https://github.com/pcw8531/thermodynamic-motor-control under MIT licence (archived at Zenodo [81]).

Electronic supplementary material is available online [82].

Declaration of AI use. I have not used AI-assisted technologies in creating this article.

Author contributions. C.P.: conceptualization, data curation, formal analysis, funding acquisition, investigation, methodology, visualization, writing—original draft, writing—review and editing.

Conflict of interest declaration. I declare I have no competing interests.

Funding. This work was supported by the Basic Science Research Program through the National Research Foundation of Korea (NRF), funded by the Ministry of Education (grant no. 2020R1I1A1A01056967; PI: C.P.). Additional support was provided by the Seoul National University BK21 Four Program.

Acknowledgements. The author thanks the members of the Center for the Ecological Study of Perception and Action (CESPA) at the University of Connecticut and the Motor Behavior Lab at Seoul National University for their invaluable support during the preparation of this article. I also express my gratitude to the participants who volunteered for this study.

References

1. Schrödinger E. 1944 *What is life?*. Cambridge, UK: Cambridge University Press. (doi:10.1017/CBO9781107295629)
2. Prigogine I, Nicolis G. 1985 Self-organisation in nonequilibrium systems: towards a dynamics of complexity. In *Bifurcation analysis* (eds M Hazewinkel, R Jurkovich, JHP Paelinck), pp. 3–12. Dordrecht, The Netherlands: Springer. (doi:10.1007/978-94-009-6239-2_1)
3. Kondepudi D, Prigogine I. 1998 *Modern thermodynamics: from heat engines to dissipative structures*. Chichester, UK: John Wiley & Sons.

4. Kleidon A, Lorenz R. 2006 Entropy production by Earth system processes. In *Non-equilibrium thermodynamics and the production of entropy: life, Earth, and beyond*, pp. 1–20. Berlin, Germany: Springer. (doi:10.1007/11672906_1)
5. Çengel YA, Boles MA. 2015 *Thermodynamics: an engineering approach*, 8th edn. New York, NY: McGraw-Hill.
6. Bauer E. 1935 *Theoretical biology* [in Russian]. Moscow, Russia: VIEM.
7. Volkenstein MV. 1982 *Physics and biology*. New York, NY: Academic Press.
8. Mizraji E. 2024 Homeostasis and information processing: the key frames for the thermodynamics of biological systems. *BioSystems* **236**, 105115. (doi:10.1016/j.biosystems.2023.105115)
9. Einstein A. 1956 *Investigations on the theory of the Brownian movement*. New York, NY: Dover.
10. Prigogine I. 1962 *Introduction to thermodynamics of irreversible processes*. New York, NY: Interscience Publishers.
11. de Groot SR, Mazur P. 1962 *Non-equilibrium thermodynamics*. Amsterdam, The Netherlands: North-Holland. (doi:10.1002/bbpc.19620661027)
12. Prigogine I, Nicolis G. 1977 *Self-organization in nonequilibrium systems: from dissipative structures to order through fluctuations*. New York, NY: Wiley.
13. Nicolis G, Prigogine I. 1989 *Exploring complexity: an introduction*. New York, NY: W. H. Freeman.
14. England JL. 2013 Statistical physics of self-replication. *J. Chem. Phys*. **139**, 121923. (doi:10.1063/1.4818538)
15. England JL. 2015 Dissipative adaptation in driven self-assembly. *Nat. Nanotechnol*. **10**, 919–923. (doi:10.1038/nnano.2015.250)
16. Haken H. 1983 *Synergetics: an introduction*, 3rd edn. Berlin, Germany: Springer-Verlag.
17. Frank TD, Daffertshofer A, Peper CE, Beek PJ, Haken H. 2001 Towards a comprehensive theory of brain activity: coupled oscillator systems under external forces. *Physica D* **144**, 62–86. (doi:10.1016/S0167-2789(00)00071-3)
18. Jaynes ET. 1957 Information theory and statistical mechanics. *Phys. Rev.* **106**, 620–630. (doi:10.1103/PhysRev.106.620)
19. Cannon WB. 1932 *The wisdom of the body*. New York, NY: Norton & Co. (doi:10.1038/133082a0)
20. Ashby WR. 1956 *An introduction to cybernetics*. London, UK: Chapman & Hall. (doi:10.1192/bjp.104.435.590-b)
21. Mizraji E, Lin J. 2011 Logic in a dynamic brain. *Bull. Math. Biol*. **73**, 373–397. (doi:10.1007/s11538-010-9561-0)
22. Haldane JBS. 1930 *Enzymes*. London, UK: Longmans, Green & Co.
23. Yates FE, Iberall AS. 1973 Temporal and hierarchical organization in biosystems. In *Temporal aspects of therapeutics* (eds J Urquhart, FE Yates), pp. 17–34. Boston, MA: Springer. (doi:10.1007/978-1-4684-2847-6_3)
24. Refinetti R, Menaker M. 1992 The circadian rhythm of body temperature. *Physiol. Behav*. **51**, 613–637. (doi:10.1016/0031-9384(92)90188-8)
25. Krauchi K, Wirz-Justice A. 1994 Circadian rhythm of heat production, heart rate, and skin and core temperature under unmasking conditions in men. *Am. J. Physiol. Regul. Integr. Comp. Physiol*. **267**, R819–R829. (doi:10.1152/ajpregu.1994.267.3.r819)
26. Gould PD *et al*. 2006 The molecular basis of temperature compensation in the Arabidopsis circadian clock. *Plant Cell* **18**, 1177–1187. (doi:10.1105/tpc.105.039990)
27. Haken H, Kelso JAS, Bunz H. 1985 A theoretical model of phase transitions in human hand movements. *Biol. Cybern.* **51**, 347–356. (doi:10.1007/BF00336922)
28. Kelso JAS. 1995 *Dynamic patterns: the self-organization of brain and behavior*. Cambridge, MA: MIT Press.
29. Park C. 2022 Eigenproperties of perception (dynamic touch) and action (phase dynamic) out of diversities. *Hum. Mov. Sci*. **85**, 102999. (doi:10.1016/j.humov.2022.102999)
30. Turvey MT, Carello C. 2012 On intelligence from first principles: guidelines for inquiry into the hypothesis of physical intelligence (PI). *Ecol. Psychol*. **24**, 3–32. (doi:10.1080/10407413.2012.645757)
31. Shannon CE. 1948 A mathematical theory of communication. *Bell Syst. Tech. J*. **27**, 379–423. (doi:10.1002/j.1538-7305.1948.tb01338.x)
32. Woodward PM. 1953 *Probability and information theory, with applications to radar*. London, UK: Pergamon Press.
33. Kharkevich AA. 1960 On the value of information. *Probl. Cybern*. **4**, 1193–1198.
34. Atkinson G, Reilly T. 1996 Circadian variation in sports performance. *Sports Med*. **21**, 292–312. (doi:10.2165/00007256-199621040-00005)
35. Edwards BJ, Atkinson G, Waterhouse J, Reilly T, Godfrey R, Budgett R. 2007 Use of melatonin in recovery from jet-lag following an eastward flight across 10 time-zones. *Ergonomics* **50**, 1676–1684. (doi:10.1080/00140130075003934)
36. Waterhouse J, Drust B, Weinert D, Edwards B, Gregson W, Atkinson G, Kao S, Aizawa S, Reilly T. 2005 The circadian rhythm of core temperature: origin and some implications for exercise performance. *Chronobiol. Int.* **22**, 207–225. (doi:10.1081/cbi-200053477)
37. Schmidt RC, Richardson MJ. 2008 Dynamics of Interpersonal Coordination. In *Coordination: neural, behavioral and social dynamics* (eds A Fuchs, VK Jirsa), pp. 281–308. Berlin, Germany: Springer. (doi:10.1007/978-3-540-74479-5_14)
38. Drust B, Waterhouse J, Atkinson G, Edwards B, Reilly T. 2005 Circadian rhythms in sports performance—an update. *Chronobiol. Int.* **22**, 21–44. (doi:10.1081/cbi-200041039)
39. Racinais S. 2010 Different effects of heat exposure upon exercise performance in the morning and afternoon. *Scand. J. Med. Sci. Sports* **20**, 80–89. (doi:10.1111/j.1600-0838.2010.01212.x)
40. Atkinson G, Drust B, Reilly T, Waterhouse J. 2007 The relevance of melatonin to sports medicine and science. *Sports Med*. **33**, 809–831. (doi:10.2165/00007256-200333110-00003)
41. Kelso JAS, DelColle JD, Schöner G. 1990 Action-perception as a pattern formation process. In *Attention and performance*, vol. XIII (ed. M Jeannerod), pp. 139–169. Hillsdale, NJ: Lawrence Erlbaum. (doi:10.4324/9780203772010-5)
42. Jirsa VK, Scott Kelso JA. 1998 The excitator as a minimal model for the coordination dynamics of discrete and rhythmic movement generation. *J. Mot. Behav*. **30**, 89–96. (doi:10.3200/jmbr.37.1.35-51)
43. Fuchs A, Jirsa VK, Haken H, Kelso JS. 1996 Extending the HKB model of coordinated movement to oscillators with different eigenfrequencies. *Biol. Cybern.* **74**, 21–30. (doi:10.1007/BF00199134)
44. Stergiou N, Harbourne RT, Cavanaugh JT. 2006 Optimal movement variability. *J. Neurol. Phys. Ther*. **30**, 120–129. (doi:10.1097/01.npt.0000281949.48193.d9)
45. Davids K, Glazier P, Araújo D, Bartlett R. 2003 Movement systems as dynamical systems. *Sports Med.* **33**, 245–260. (doi:10.2165/00007256-200333040-00001)
46. Riley MA, Turvey MT. 2002 Variability and determinism in motor behavior. *J. Mot. Behav*. **34**, 99–125. (doi:10.1080/00222890209601934)
47. Scholz JP, Schöner G. 1999 The uncontrolled manifold concept: identifying control variables for a functional task. *Exp. Brain Res*. **126**, 289–306. (doi:10.1007/s002210050738)
48. Turvey MT. 1990 Coordination. *Am. Psychol.* **45**, 938–953.
49. Ashby WR. 1954 *Design for a brain: the origin of adaptive behavior*. New York, NY: John Wiley & Sons.
50. West BJ, Griffin LA, Frederick HJ, Moon RE. 2002 The independently fractal nature of respiration and heart rate during exercise under normobaric and hyperbaric conditions. *Respir. Physiol. Neurobiol.* **145**, 219–233. (doi:10.1016/j.resp.2004.07.010)
51. Lipsitz LA. 2002 Dynamics of stability: the physiologic basis of functional health and frailty. *J. Gerontol. Ser*. **57**, B115–B125. (doi:10.1093/gerona/57.3.b115)

52. Sleimen-Malkoun R, Temprado JJ, Hong SL. 2014 Aging induced loss of complexity and dedifferentiation: consequences for coordination dynamics within and between brain, muscular and behavioral levels. *Front. Aging Neurosci*. **6**, 140. (doi:10.3389/fnagi.2014.00140)
53. Friston K. 2010 The free-energy principle: a unified brain theory? *Nat. Rev. Neurosci.* **11**, 127–138. (doi:10.1038/nrn2787)
54. Seely AJE, Macklem PT. 2004 Complex systems and the technology of variability analysis. *Crit. Care* **8**, R367–R384. (doi:10.1186/cc2948)
55. Amazeen EL, Amazeen PG, Treffner PJ, Turvey MT. 1997 Attention and handedness in bimanual coordination dynamics. *J. Exp. Psychol.* **23**, 1552–1560. (doi:10.1037/0096-1523.23.5.1552)
56. Faul F, Erdfelder E, Lang AG, Buchner A. 2007 G*Power 3: a flexible statistical power analysis program for the social, behavioral, and biomedical sciences. *Behav. Res. Methods* **39**, 175–191. (doi:10.3758/bf03193146)
57. Cohen J. 1992 Quantitative methods in psychology: a power primer. *Psychol. Bull.* **112**, 155–159. (doi:10.1037//0033-2909.112.1.155)
58. Aschoff J. 1983 Circadian control of body temperature. *J. Therm. Biol.* **8**, 143–147. (doi:10.1016/0306-4565(83)90094-3)
59. Weinert D, Waterhouse J. 1998 Diurnally changing effects of locomotor activity on body temperature in laboratory mice. *Physiol. Behav.* **63**, 837–843. (doi:10.1016/s0031-9384(97)00546-5)
60. Kräuchi K. 2001 Circadian clues to sleep onset mechanisms. *Neuropsychopharmacology* **25**, S5. (doi:10.1016/s0893-133x(01)00315-3)
61. Pikovsky A, Rosenblum M, Kurths J. 2001 *Synchronization: a universal concept in nonlinear sciences*. Cambridge, UK: Cambridge University Press. (doi:10.1017/CBO9780511755743)
62. Stergiou N, Decker LM. 2011 Human movement variability, nonlinear dynamics, and pathology: is there a connection? *Hum. Mov. Sci*. **30**, 869–888. (doi:10.1016/j.humov.2011.06.002)
63. Schneider ED, Kay JJ. 1994 Life as a manifestation of the second law of thermodynamics. *Math. Model. Comput.* **19**, 25–48. (doi:10.1016/0895-7177(94)90188-0)
64. Kleidon A. 2009 Nonequilibrium thermodynamics and maximum entropy production in the Earth system. *Naturwissenschaften* **96**, 653–677. (doi:10.1007/s00114-009-0509-x)
65. Callen HB. 1985 *Thermodynamics and an introduction to thermostatistics*, 2nd edn. New York, NY: John Wiley & Sons.
66. Schneider ED, Sagan D. 2005 *Into the cool: energy flow, thermodynamics, and life*. Chicago, IL: University of Chicago Press.
67. Crooks GE. 1999 Entropy production fluctuation theorem and the nonequilibrium work relation for free energy differences. *Phys. Rev. E* **60**, 2721–2726. (doi:10.1103/physreve.60.2721)
68. Soodak H, Iberall A. 1978 Homeokinetics: a physical science for complex systems. *Science* **201**, 579–582. (doi:10.1126/science.201.4356.579)
69. Boyer PD. 1997 The ATP synthase—a splendid molecular machine. *Annu. Rev. Biochem.* **66**, 717–749. (doi:10.1146/annurev.biochem.66.1.717)
70. Henzler-Wildman KA, Lei M, Thai V, Kerns SJ, Karplus M, Kern D. 2007 A hierarchy of timescales in protein dynamics is linked to enzyme catalysis. *Nature* **450**, 913–916. (doi:10.1038/nature06407)
71. Kao MH, Doupe AJ, Brainard MS. 2005 Contributions of an avian basal ganglia–forebrain circuit to real-time modulation of song. *Nature* **433**, 638–643. (doi:10.1038/nature03127)
72. Harrison SJ, Stergiou N. 2015 Complex adaptive behavior and dexterous action. *Nonlinear. Dyn. Psychol. Life Sci.* **19**, 345–394.
73. Vaillancourt DE, Newell KM. 2002 Changing complexity in human behavior and physiology through aging and disease. *Neurobiol. Aging* **23**, 1–11. (doi:10.1016/s0197-4580(01)00247-0)
74. West GB. 2006 Size, scale, and the boat race: conceptions, connections, and misconceptions. In *Hierarchy in natural and social sciences* (ed. D Pumain), vol. **3**. Dordrecht, The Netherlands: Springer.(Methodos Series). (doi:10.1007/1-4020-4127-6_4)
75. Clarke A, Rothery P. 2008 Scaling of body temperature in mammals and birds. *Funct. Ecol*. **22**, 58–67. (doi:10.1111/j.1365-2435.2007.01341.x)
76. Kaila VR, Annila A. 2008 Natural selection for least action. *Proc. R. Soc. A* **464**, 3055–3070. (doi:10.1098/rspa.2008.0178)
77. Nagel DH, Pruneda-Paz JL, Kay SA. 2014 FBH1 affects warm temperature responses in the Arabidopsis circadian clock. *Proc. Natl Acad. Sci. USA* **111**, 14595–14600. (doi:10.1073/pnas.1416666111)
78. Todorov E, Jordan MI. 2002 Optimal feedback control as a theory of motor coordination. *Nat. Neurosci*. **5**, 1226–1235. (doi:10.1038/nn963)
79. Corning PA, Kline SJ. 1998 Thermodynamics, information and life revisited. Part I. 'To be or entropy'. *Syst. Res. Behav. Sci.* **15**, 273–295. (doi:10.1002/(sici)1099-1743(199807/08)15:43.0.co;2-b)
80. Pascal R, Pross A, Sutherland JD. 2013 Towards an evolutionary theory of the origin of life based on kinetics and thermodynamics. *Open Biol.* **3**, 130156. (doi:10.1098/rsob.130156)
81. Park C. 2026 pcw8531/thermodynamic-motor-control: v1.0—publication release (v1.0). Zenodo. (doi:10.5281/zenodo.19201270)
82. Park C. 2026 Supplementary material from: thermodynamic entropy management in human motor control across circadian and thermal challenges. Figshare. (doi:10.6084/m9.figshare.c.8463251)